JACS
JOURNAL OF THE AMERICAN CHEMICAL SOCIETY
Article
pubs.acs.org/JACS

Mechanical Bond-Induced Radical Stabilization

Hao Li, Zhixue Zhu, Albert C. Fahrenbach, Brett M. Savoie, Chenfeng Ke, Jonathan C. Barnes, Juying Lei, Yan-Li Zhao, Laura M. Lilley, Tobin J. Marks, Mark A. Ratner, and J. Fraser Stoddart*

Department of Chemistry, Northwestern University, 2145 Sheridan Road, Evanston, Illinois 60208-3113, United States

Supporting Information

ABSTRACT: A homologous series of [2]rotaxanes, in which cyclobis(paraquat-*p*-phenylene) ($CBPQT^{4+}$) serves as the ring component, while the dumbbell components all contain single 4,4′-bipyridinium ($BIPY^{2+}$) units centrally located in the midst of oligomethylene chains of varying lengths, have been synthesized by taking advantage of radical templation and copper-free azide−alkyne 1,3-dipolar cycloadditions in the formation of their stoppers. Cyclic voltammetry, UV/vis spectroscopy, and mass spectrometry reveal that the $BIPY^{\bullet+}$ radical cations in this series of [2]rotaxanes are stabilized against oxidation, both electrochemically and by atmospheric oxygen. The enforced proximity between the $BIPY^{2+}$ units in the ring and dumbbell components gives rise to enhanced Coulombic repulsion, destabilizing the ground-state co-conformations of the fully oxidized forms of these [2]rotaxanes. The smallest [2]rotaxane, with only three methylene groups on each side of its dumbbell component, is found to exist under ambient conditions in a monoradical state, a situation which does not persist in acetonitrile solution, at least in the case of its longer analogues. ^{1}H NMR spectroscopy reveals that the activation energy barriers to the shuttling of the $CBPQT^{4+}$ rings over the $BIPY^{2+}$ units in the dumbbells increase linearly with increasing oligomethylene chain lengths across the series of [2]rotaxanes. These findings provide a new way of producing highly stabilized $BIPY^{\bullet+}$ radical cations and open up more opportunities to use stable organic radicals as building blocks for the construction of paramagnetic materials and conductive molecular electronic devices.

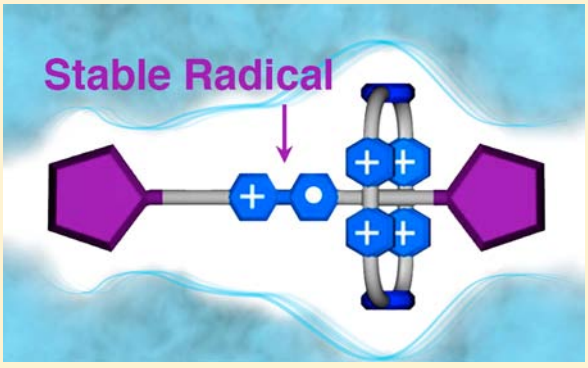

INTRODUCTION

In the fields of supramolecular chemistry[1] and mechanostereochemistry,[2] 4,4′-bipyridinium[3] ($BIPY^{2+}$) units and cyclobis(paraquat-*p*-phenylene)[4] ($CBPQT^{4+}$)—a rigid tetracationic cyclophane with two $BIPY^{2+}$ units locked in place at 7 Å apart—have been investigated extensively as a π-electron-deficient guest and host, respectively. Although these building blocks have been employed in the design and synthesis of host−guest inclusion complexes and as components in mechanically interlocked molecules[5] (MIMs), including catenanes[6] and rotaxanes,[7] only rarely have they been the two sole recognition units united together in the context of the mechanical bond. In the majority of examples to date, the syntheses of these MIMs have been based on templation protocols which involve noncovalent π-electron donor−acceptor[8] interactions between $BIPY^{2+}$ units and π-electron-rich moieties, e.g., tetrathiafulvalene[9] and 1,5-dioxynaphthalene[10] ring systems. These stabilizing π-electronic forces are often assisted by [C−H···O] interactions[11] which occur between the relatively acidic protons in the α-positions of $BIPY^{2+}$ units as hydrogen bond donors and acceptors, such as the oxygen atoms associated with polyether chains in rings or dumbbells.

In stark contrast with $BIPY^{2+}$ units, which act as π-electron acceptors in their fully oxidized dicationic states, the reduced radical-cationic forms—namely $BIPY^{\bullet+}$—of $BIPY^{2+}$ dications express a strong tendency to undergo pimerization,[12] in which two or more $BIPY^{\bullet+}$ units come together in a face-to-face manner to form $(BIPY^{\bullet+})_2$ radical π-dimers, or "pimers".[12a] The formation of $(BIPY^{\bullet+})_2$ radical dimers is driven in large part by the free energy obtained from the pairing of their unpaired π-electrons. This process, however, is entropically unfavorable,[12a] resulting in the $(BIPY^{\bullet+})_2$ radical dimers undergoing dissociation into $BIPY^{\bullet+}$ monomers in the absence of preorganization.

One of the approaches favoring $(BIPY^{\bullet+})_2$ dimer formation in solution is to construct synthetically a cage—or, expressed another way, a so-called[13] "molecular flask"—as a means of organizing the enforced association of the radicals. For example, Kim and co-workers[14] demonstrated that the stability of a $(BIPY^{\bullet+})_2$ radical dimer can be enhanced when it is encapsulated within cucurbit[8]uril. Recently, we observed[15] that the $CBPQT^{2(\bullet+)}$ ring itself has the ability to form stable trisradical tricationic $BIPY^{\bullet+}\subset CBPQT^{2(\bullet+)}$ inclusion complexes with $BIPY^{\bullet+}$ units, where the $CBPQT^{2(\bullet+)}$ ring provides a preorganized cavity wherein the $BIPY^{\bullet+}$ guests can undergo[16] efficient $\pi-\pi$ stacking with both $BIPY^{\bullet+}$ units of the $CBPQT^{2(\bullet+)}$ ring. While in one instance these radical-pairing interactions have been employed[17] successfully as a novel recognition motif to template the formation of a [2]rotaxane,

Received: October 11, 2012
Published: November 19, 2012

   dx.doi.org/10.1021/ja310060n | J. Am. Chem. Soc. 2013, 135, 456−467

the redox-activated bistability of $BIPY^{\bullet+}$ units also affords these compounds opportunities to become integrated into nano-electromechanical systems[18] (NEMs). In addition, the radical nature of $BIPY^{\bullet+}$ units can lead to functional composite materials with a variety of potential applications, e.g., paramagnetic materials[19] and conductive molecular electronic devices.[20] However, these potential applications have remained, for the most part, unexplored, probably at least in part on account of the low resistance of $BIPY^{\bullet+}$ radical cations to oxidation by atmospheric O_2. Consequently, finding ways to increase the stability of these radical cations toward atmospheric O_2 remains a major challenge in radical chemistry.

In this article, we report the results of an investigation relating to the impact of the mechanically interlocked nature of a homologous series of [2]rotaxanes **R*n***·$6PF_6$ (n = 3−11, which represents the number of the methylene groups on each side of the central $BIPY^{2+}$ unit in the dumbbell components) on their structural, electronic, and spectroscopic properties. These [2]rotaxanes each consist of a $CBPQT^{4+}$ ring encircling a dumbbell containing only one central $BIPY^{2+}$ unit with a range of oligomethylene chain lengths. We discuss how we have investigated (i) the activation energy barriers to the shuttling of $CBPQT^{4+}$ rings over the $BIPY^{2+}$ dicationic units, which serve as electrostatic "speed bumps",[17] in the middle of the dumbbells by dynamic ^{1}H NMR spectroscopy and (ii) the electronic stability of the radical states of these [2]rotaxanes toward oxidation, employing cyclic voltammetry (CV), UV/vis spectroscopy, and mass spectrometry. The results reveal that the mechanical bonds associated with these [2]rotaxanes lead to the enforced proximity between the mechanically interlocked components in their ground state co-conformations (GSCCs) and thereby have a significant impact on their molecular properties, e.g., the activation energy barriers to the shuttling of the rings along the corresponding dumbbells and the stability of their radical states toward oxidation. The progressive enhancement of the stability of the $BIPY^{\bullet+}$ radical cations under atmospheric oxygen, as a function of decreasing oligomethylene chain length, leads to the formation of a monoradical state in the case of the smallest [2]rotaxane, namely **R3**$^{6+}$. These results presage a new methodology for the synthesis of stable organic radicals taking advantage of mechanical bonds.

RESULTS AND DISCUSSION

The observation[15] that $BIPY^{\bullet+}$ radical cationic guests can form stable inclusion complexes with the diradical dicationic $CBPQT^{2(\bullet+)}$ ring, as a consequence of stabilizing radical−radical interactions—a large part of which is brought about[15] by the pairing of electrons in the $BIPY^{\bullet+}$ radical cations—has been utilized[17] previously in the template-directed synthesis of the [2]rotaxane **R′11**·$6PF_6$. (See Figure 1a for its structural formula. The descriptor **R′** implies that the [2]rotaxane **R′11**·$6PF_6$ contains relatively smaller stoppers—compared to those present in the [2]rotaxanes **R3**·$6PF_6$−**R11**·$6PF_6$—bearing two *tert*-butyl groups on the ester functions of the triazole rings.) After oxidation, on account of the resulting Coulombic repulsion between the $BIPY^{2+}$ units in the dumbbell and ring, the fully oxidized [2]rotaxane **R′11**·$6PF_6$ occupies a much higher energy state when compared with the corresponding free components. The disassociation of these two components in **R′11**·$6PF_6$ is prohibited by the presence of the bulky stoppers in the dumbbell of the [2]rotaxane **R′11**·$6PF_6$.

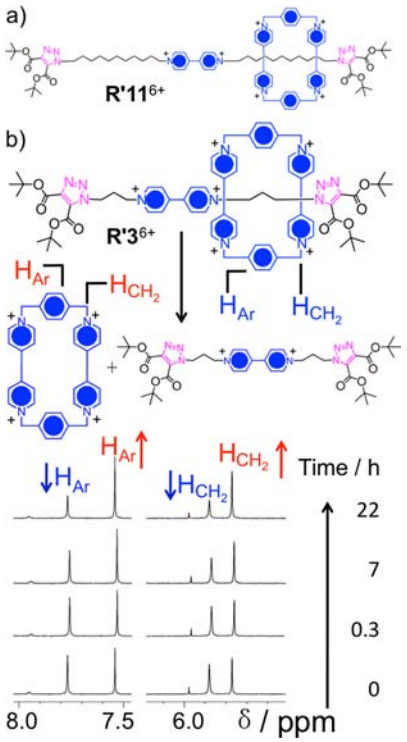

Figure 1. (a) Structural formula of the [2]rotaxane **R′11**·$6PF_6$. (b) Partial ^{1}H NMR spectra of **R′3**·$6PF_6$ (600 MHz, CD_3CN), illustrating the kinetics of the dethreading of **R′3**·$6PF_6$ at 318 K. The resonances of the $CBPQT^{4+}$ ring component of **R′3**·$6PF_6$ are marked with blue arrows, while those of the "free" $CBPQT^{4+}$ are marked with red arrows.

In order to gain a deeper understanding of the impact of the mechanical bond on the properties of this series of [2]rotaxanes obtained by radical templation, we pursued the synthesis of **R′3**·$6PF_6$ (see Figure 1b for its structural formula), a shorter analogue of the [2]rotaxane **R′11**·$6PF_6$, which has only three methylene units—instead of 11 in the case of **R′11**·$6PF_6$—on each side of the $BIPY^{2+}$ unit in its dumbbell component. It transpires that **R′3**$^{6+}$ undergoes decomposition into its free dumbbell and ring at room temperature as a result of Coulombic repulsion between its two positively charged components, implying that **R′3**$^{6+}$ is neither a thermodynamically nor a kinetically stable compound.[21] The representative parts of the ^{1}H NMR spectra showing the kinetics of the decomposition of **R′3**$^{6+}$ at 318 K are recorded in Figure 1. In the course of time, we observed that the resonances of the threaded ring in **R′3**$^{6+}$ decreased, while those of the free dumbbell and ring increased. The decomposition of **R′3**$^{6+}$ takes place in a manner whereby the $CBPQT^{4+}$ ring dethreads (deslips) from the dumbbell, rather than any cleavage of covalent bonds occurring in either the dumbbell or ring components. The implication is that, in contrast with the [2]rotaxane **R′11**$^{6+}$, **R′3**$^{6+}$ behaves essentially like a pseudo-rotaxane, at least in its oxidized form, even though the compositions of their stoppers are identical.[22] The difference in the behavior of the two rotaxanes results from the fact that, in the fully oxidized state of **R′3**$^{6+}$, the enforced proximity between the $CBPQT^{4+}$ ring and the $BIPY^{2+}$ unit in the middle of the dumbbell component is greatly enhanced compared to that in **R′11**$^{6+}$. This enforced proximity increases Coulombic repulsion, activating the ring to pass over one of the two bulky

dx.doi.org/10.1021/ja310060n | J. Am. Chem. Soc. 2013, 135, 456−467

stoppers, i.e., the energy barrier for this dethreading process becomes reduced as a result of the destabilization of the GSCC.

Further ^{1}H NMR spectroscopy was used to investigate the kinetics of dethreading of $\mathbf{R'3}^{6+}$ at two additional temperatures, 313 and 323 K. On the basis of these data, the rate constants, k, for the dethreading of $\mathbf{R'3}^{6+}$ at 313, 318, and 323 K were calculated from the corresponding plots (Figure S31b) of $\ln([c]/[c]_0)$ vs time, in which $[c]$ and $[c]_0$ represent the concentrations of the $\mathbf{R'3}^{6+}$ with time and the initial concentrations, respectively. The linearity of these three plots indicates that the dethreading process is first-order at all three temperatures. An activation energy (E_a) of 32 ± 3 kcal/mol was obtained from the Arrhenius plot (Figure S31c). The E_a value corresponds to a half-life ($t_{1/2}$) for $\mathbf{R'3}^{6+}$ at room temperature of ca. 30 days. An Eyring plot (Figure S31d) reveals a $\Delta H^{\ddagger}$ of 31 ± 3 kcal/mol and a $\Delta S^{\ddagger}$ of 18 ± 2 cal/K·mol, from which a free energy $\Delta G^{\ddagger}$(298 K) of 26 kcal/mol was calculated. The positive entropy of activation indicates that the dethreading process has a less ordered transition-state co-conformation than the GSCC. In the GSCC of $\mathbf{R'3}^{6+}$, the two trimethylene chains act as the "recognition sites" for the $CBPQT^{4+}$ ring, causing the free rotation of the two trimethylene chains to be inhibited to some extent. This entropy loss in the GSCC, however, does not occur in the transition state during the dethreading of $\mathbf{R'3}^{6+}$ when the $CBPQT^{4+}$ ring encircles one of the two stoppers in the dumbbell component of $\mathbf{R'3}^{6+}$. The consequence is that the kinetics of dethreading is entropically favorable while being enthalpically unfavorable.

In order to prevent dissociation of the $CBPQT^{4+}$ ring from the dumbbell components of [2]rotaxanes, we employed (Scheme 1) a bulkier stopper bearing two 2,2-dimethylpropyl units on the ester functions of the triazole rings which are formed during the synthesis of the [2]rotaxanes. We observed that bulkier stoppers are capable of interlocking the rings mechanically on the rods of the modified [2]rotaxanes, i.e., the bulkier stoppers prohibit dethreading of the ring from the dumbbell component. A homologous series of [2]rotaxanes, $\mathbf{R3}\cdot 6PF_6$–$\mathbf{R11}\cdot 6PF_6$, which differ from each other only in the number (n) of methylene groups located on both sides of the central $BIPY^{2+}$ unit in the dumbbell components, have been synthesized (see Scheme 1 and SI for the details of the syntheses), taking advantage of radical templation[17] and a threading followed by stoppering approach. Zn dust was used[15b] to reduce the $BIPY^{2+}$ units in both the rods $\mathbf{V3}^{2+}$–$\mathbf{V11}^{2+}$ and the $\mathbf{CBPQT}^{4+}$ ring from their fully oxidized states to the $BIPY^{\bullet+}$ radical states, yielding nine 1:1 inclusion complexes $\mathbf{V3}^{\bullet+}$–$\mathbf{V11}^{\bullet+}\subset\mathbf{CBPQT}^{2(\bullet+)}$, respectively. In order to make the mechanically interlocked compounds, namely the [2]rotaxanes $\mathbf{R3}^{6+}$–$\mathbf{R11}^{6+}$, copper-free[17,23] azide–alkyne 1,3-dipolar cycloadditions[24] between the stopper precursor **S** and the terminal azide groups on the rods ($\mathbf{V3}^{\bullet+}$–$\mathbf{V11}^{\bullet+}$) were carried out.[25] The [2]rotaxanes $\mathbf{R3}\cdot 6PF_6$–$\mathbf{R11}\cdot 6PF_6$ were isolated (Figure 2) in yields[26] varying from 5% to 35% after workup, during which time all of the $BIPY^{\bullet+}$ radical cations were oxidized[27] back to $BIPY^{2+}$ dications by atmospheric O_2. All of the new [2]rotaxanes $\mathbf{R3}\cdot 6PF_6$–$\mathbf{R11}\cdot 6PF_6$ were characterized (see the SI) by NMR spectroscopy and mass spectrometry. In the case of all nine of these [2]rotaxanes, no dissociation was observed to occur at room temperature during a long period of time (i.e., of the order of weeks), even at elevated temperatures, indicating that the stoppers are bulky enough to overcome Coulombic repulsion and so prevent the dethreading of the rings from their dumbbell components.

Scheme 1. Radically Promoted, Template-Directed Syntheses of the [2]Rotaxanes $\mathbf{R3}^{6+}$–$\mathbf{R11}^{6+}$ from the [2]Pseudorotaxanes $\mathbf{V3}^{\bullet+}$–$\mathbf{V11}^{\bullet+}\subset\mathbf{CBPQT}^{2(\bullet+)}$ Which Afford the [2]Rotaxanes $\mathbf{R3}^{3(\bullet+)}$–$\mathbf{R11}^{3(\bullet+)}$ (See General Procedure D), Prior to Their Subsequent Aerobic Oxidation To Give $\mathbf{R3}^{6+}$–$\mathbf{R11}^{6+}$ during Their Purification[a]

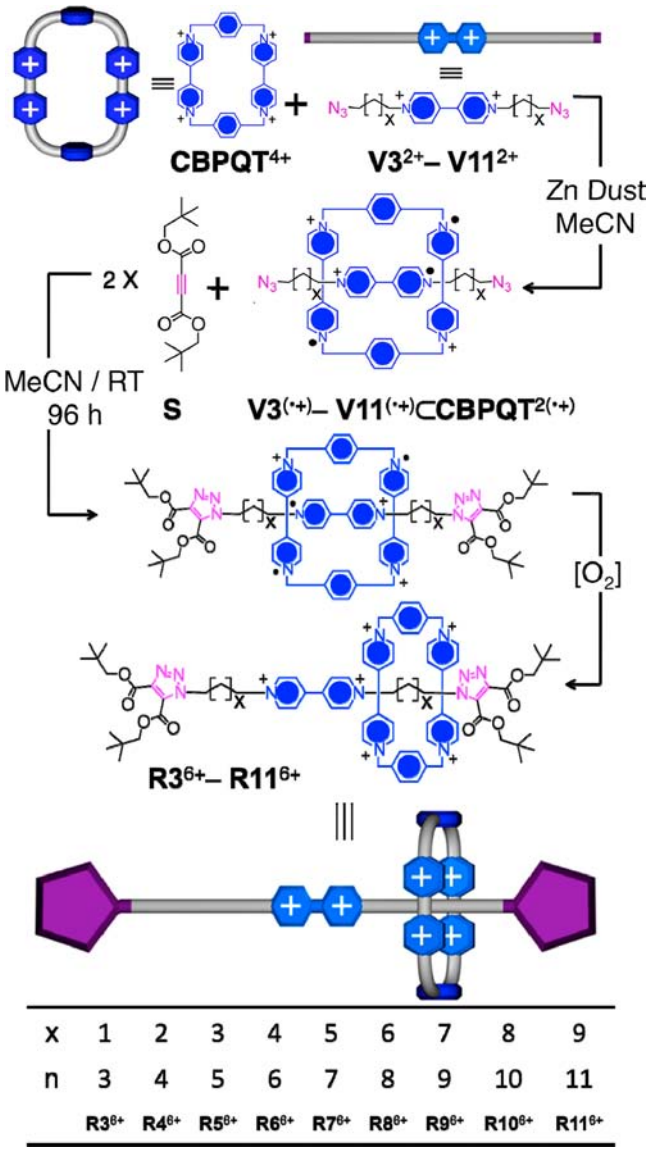

[a]The PF_6^- counterions are omitted for the sake of clarity.

The $CBPQT^{4+}$ rings in all these [2]rotaxanes undergo shuttling along the length of their respective dumbbells from one end to the other. The $BIPY^{2+}$ units in the middle of the dumbbell components slow down the shuttling process by introducing Coulombic repulsion to passage of the $CBPQT^{4+}$ rings, given that both the $BIPY^{2+}$ unit and the $CBPQT^{4+}$ ring are carrying a total of six formal positive charges between them. Variable temperature (VT) ^{1}H NMR spectroscopy (see the SI) has been employed to investigate the shuttling characteristics of the [2]rotaxanes. Using the Eyring equation, the activation energy barriers ($\Delta G^{\ddagger}_{\text{shuttling}}$) for the shuttling of the $CBPQT^{4+}$ rings along the dumbbell components of the [2]rotaxanes have been calculated[28] from the limiting chemical shifts ($\Delta\nu$) and the coalescence temperatures, both of which can be probed (see the SI) by VT ^{1}H NMR spectroscopy. In the case of both

dx.doi.org/10.1021/ja310060n | J. Am. Chem. Soc. 2013, 135, 456–467

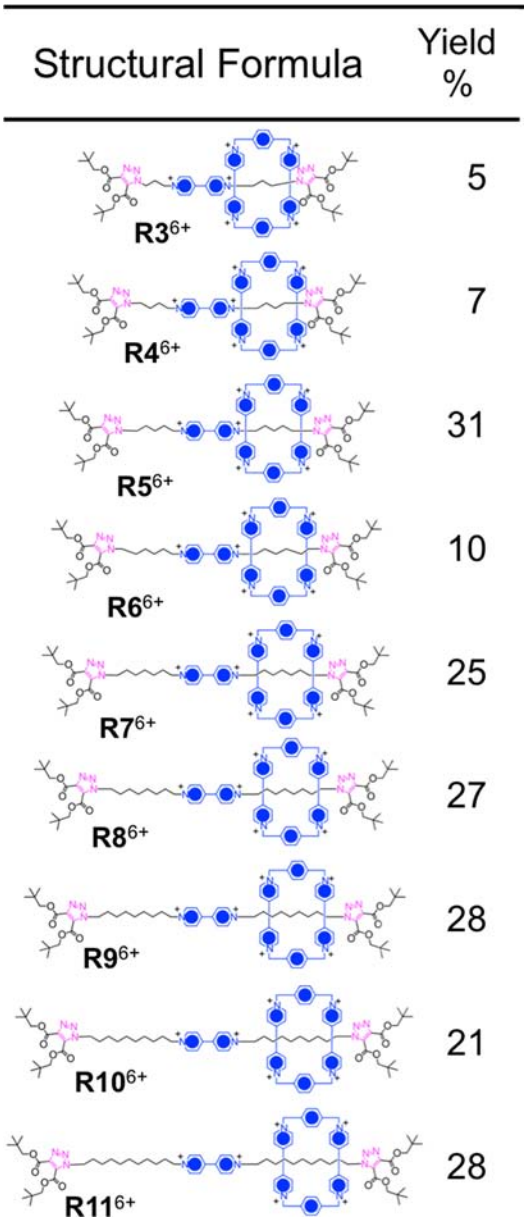

Figure 2. Structural formulas and percentage yields of the last steps of the radically promoted, template-directed syntheses of the [2]-rotaxanes **R3**$^{6+}$–**R11**$^{6+}$. The PF_6^- counterions are omitted for the sake of clarity.

R10^{6+} and **R11**$^{6+}$, coalescence behavior was not observed anywhere in the ^{1}H NMR spectra recorded in CD_3COCD_3, even at 330 K, a temperature close to the boiling point of the solvent. This observation indicates that the values of $\Delta G^{\ddagger}_{shuttling}$ for the [2]rotaxanes **R10**$^{6+}$ and **R11**$^{6+}$ at 330 K in CD_3COCD_3 must be greater than ~16 kcal/mol. The shuttling of the CBQPT^{4+} rings is relatively slow on the NMR time scale, an observation which is consistent with previous results.[17] In the case of the [2]rotaxanes **R3**$^{6+}$–**R9**$^{6+}$, the values of $\Delta G^{\ddagger}_{shuttling}$ were found to be 11.4, 12.3, 12.7, 13.7, 14.6, 15.4, and 15.8 kcal/mol, respectively. $\Delta G^{\ddagger}_{shuttling}$ increases linearly (Figure 3a) with increasing oligomethylene chain lengths in the [2]-rotaxanes, an observation which is best explained by the changes in the proximity between the two mechanically interlocked components in the [2]rotaxanes. In the fully oxidized states, compared to the longer [2]rotaxanes, the

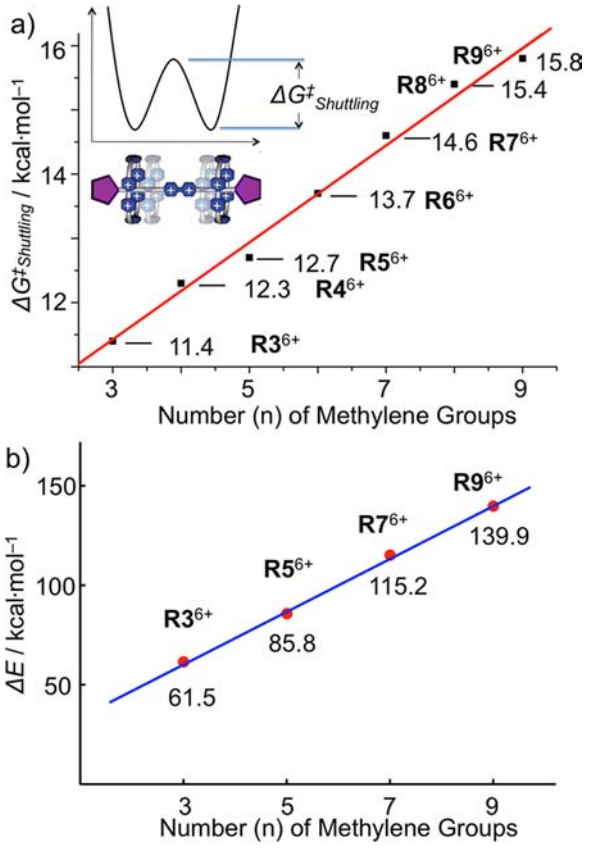

Figure 3. (a) Plot of the activation energy barriers ($\Delta G^{\ddagger}_c$) associated with the CBQPT^{4+} rings passing over the BIPY^{2+} units in the middle of the corresponding dumbbell components in the [2]rotaxanes **R***n*·6PF_6 (*n* = 3–9) versus the number (*n*) of methylene groups in the polymethylene chains on each side of the BIPY^{2+} units in the dumbbell components of the [2]rotaxanes **R***n*·6PF_6. (b) Activation energy barriers (ΔE) for the **CBPQT**$^{4+}$ ring components to shuttle over the **BIPY**$^{2+}$ units in the corresponding dumbbell components of the [2]rotaxanes **R3**$^{6+}$, **R5**$^{6+}$, **R7**$^{6+}$, and **R9**$^{6+}$, which are obtained from DFT calculations (see SI for the details of the general calculation methods).

CBPQT^{4+} rings in shorter [2]rotaxanes reside in positions that are closer to the BIPY^{2+} units in the middle of their dumbbells, and thereby undergo larger Coulombic repulsion, conferring higher energy states upon their GSCCs. As a consequence, the activation energy barriers for the shuttling process of shorter [2]rotaxanes are reduced (Figure 3a). These results are consistent with density functional theory (DFT) calculations (Figure 3b), which also reveal (see the SI) a decrease in the activation energy barriers in the case of shorter [2]rotaxanes, because of the destabilization of their GSCCs.[29]

The electrochemical behavior of the [2]rotaxanes **R3**$^{6+}$–**R11**$^{6+}$ was investigated by CV. The CV traces of the [2]rotaxanes, with the exception of **R3**$^{6+}$, reveal (see the SI and Figure 4) four consecutive reversible redox processes. The potential for the first reduction peaks varies from −0.01 to −0.16 V. The first redox process can be assigned to two simultaneous one-electron reductions: one electron being transferred to one of the BIPY^{2+} units of the CBPQT^{4+} ring to give CBPQT$^{(2+)(\bullet+)}$ from CBPQT^{4+}, and the other to the BIPY^{2+} unit of the dumbbell component (BIPY^{2+}/BIPY$^{\bullet+}$). A significant positive shift, e.g., −0.01 V for **R4**$^{6+}$ (see the SI) and −0.16 V for **R11**$^{6+}$ (Figure 4b), of the first reduction peaks is

dx.doi.org/10.1021/ja310060n | J. Am. Chem. Soc. 2013, 135, 456–467

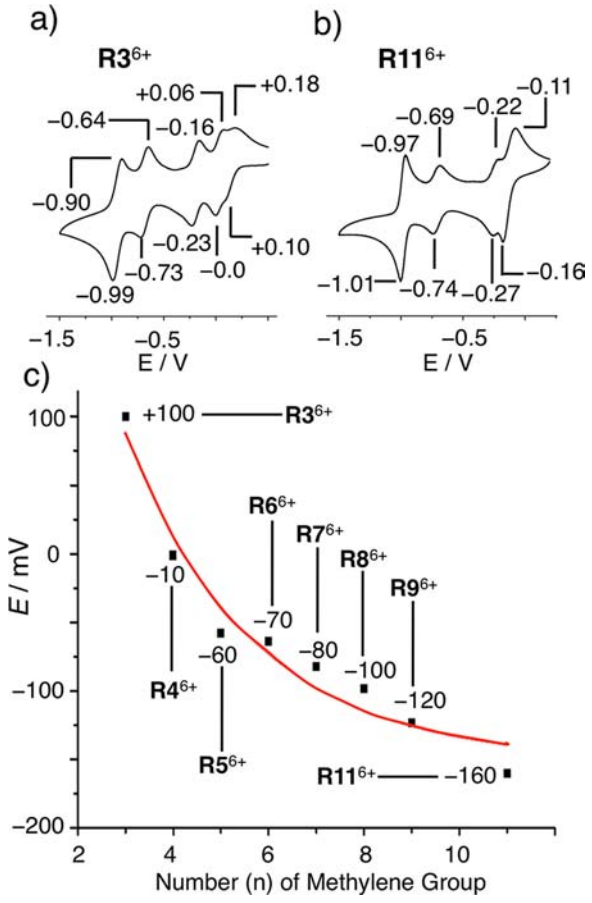

Figure 4. Cyclic voltammograms of the [2]rotaxanes: (a) **R3**·6PF_6 and (b) **R11**·6PF_6. The CV spectra were recorded at 298 K in argon-purged MeCN (1 mM) and electrolyte TBA·PF_6 (0.1 M). The scan rate was set at 200 mV s^{-1}. (c) Plot of the first reduction peak potentials in the CV spectra of **R3**·6PF_6–**R11**·6PF_6 (excluding **R10**·6PF_6) versus the number (n) of methylene groups in the polymethylene chains on each side of the $BIPY^{2+}$ units in the dumbbell components of the [2]rotaxanes **R***n*·6PF_6.

observed (Figure 4c) with a decreasing number of methylene groups present in the oligomethylene linkers in the [2]-rotaxanes. This observation can be attributed to the fact that, in the fully oxidized state of the shorter [2]rotaxanes, the enhanced proximities between the $BIPY^{2+}$ units in the dumbbells and the $CBPQT^{4+}$ rings introduce larger Coulombic repulsions between these two positively charged components, raising the shorter [2]rotaxanes to relatively higher energy levels compared to their longer analogues. As a result, the shorter [2]rotaxanes have a higher tendency to undergo the first two-electron reductions, a trend which decreases Coulombic repulsion and introduces stabilizing radical-pairing interactions between the mechanically interlocked components. The reduction peaks for all nine [2]rotaxanes, including $\mathbf{R3}^{6+}$, observed around −0.25 V and corresponding to one-electron processes, can be attributed to the further reduction of the $CBPQT^{(2+)(\bullet+)}$ monoradical trication to its $CBPQT^{2(\bullet+)}$ diradical dicationic state. The third reduction peaks, observed around −0.70 V for these [2]rotaxanes, can be assigned to the one-electron reduction of one of the two $BIPY^{\bullet+}$ units in the $CBPQT^{2(\bullet+)}$ ring ($CBPQT^{2(\bullet+)}$/$CBPQT^{\bullet+}$), which is not as strongly engaged in radical–radical interactions with the $BIPY^{\bullet+}$ radical cation of the dumbbell components of the [2]rotaxanes. The fourth reduction peaks, observed around −1.0 V, can be attributed to two simultaneous one-electron reductions, namely $CBPQT^{\bullet+}$/CBPQT and $BIPY^{\bullet+}$/BIPY. These results are consistent with previously published results.[16] It is noteworthy that all of the reduction processes, except the first two-electron ones, do not display a marked dependence on the lengths of the rotaxanes. This observation can be explained by the fact that, after the first two-electron reductions, the $CBPQT^{(2+)(\bullet+)}$ rings move and reside on the $BIPY^{\bullet+}$ units in the middle of the dumbbell components, and so the proximity or otherwise of the stoppers does not have a strong effect on radical–radical interactions. In a nutshell, all nine [2]rotaxanes, after the first two-electron reductions, have similar electronic properties, regardless of the lengths of the oligomethylene chains present within their dumbbell components.

In contrast with its longer counterparts, which all undergo simultaneous first two-electron reductions, the [2]rotaxane $\mathbf{R3}^{6+}$ undergoes two one-electron reductions in a stepwise manner. The first and second reduction peaks of the [2]rotaxane $\mathbf{R3}^{6+}$, observed (Figure 4a) at +0.10 and 0.00 V, can be assigned[30] to two stepwise one-electron reductions: one electron being transferred to the $BIPY^{2+}$ unit of the dumbbell component ($BIPY^{2+}$/$BIPY^{\bullet+}$), and the other to one of the $BIPY^{2+}$ units of the $CBPQT^{4+}$ ring ($CBPQT^{4+}$/$CBPQT^{(2+)(\bullet+)}$). The potentials of these two one-electron reduction peaks for the [2]rotaxane $\mathbf{R3}^{6+}$ also show a positive shift (Figure 4a) compared to those for $\mathbf{R4}^{6+}$–$\mathbf{R11}^{6+}$, indicating that, among these nine [2]rotaxanes, $\mathbf{R3}^{6+}$ has the highest tendency to undergo these reductions. Expressed another way, the diradical state of $\mathbf{R3}^{6+}$, namely $\mathbf{R3}^{(2+)2(\bullet+)}$, has the highest resistance to oxidation. The stepwise two-electron reduction implies that the [2]rotaxane $\mathbf{R3}^{6+}$ has a monoradical state, namely $\mathbf{R3}^{(4+)(\bullet+)}$, an observation which is consistent with previously unpublished results.[31]

In order to shed further light on the reason why $\mathbf{R3}^{6+}$ has a stabilized monoradical state while its longer analogues do not, DFT calculations were performed to evaluate and compare the energies of the [2]rotaxane $\mathbf{R3}^{6+}$ with one of its longer counterparts, namely $\mathbf{R5}^{6+}$ in both their fully oxidized and monoradical states. According to the results of these calculations, both of these [2]rotaxanes favor the formation (Figure 5) of the monoradical states compared to their fully oxidized forms in a vacuum. This preferemce for the monoradical states occurs on account of the smaller number of positive charges significantly reducing the Coulombic repulsion between the positively charged $BIPY^{2+}$ units in the ring and dumbbell components. These calculations are consistent with the results of mass spectrometry, i.e., **R3**·6PF_6 (Figure S30), as well as its longer analogues, including **R4**·6PF_6 (Figure S31a) and **R6**·6PF_6 (Figure S31b), which possess[32] stabilized monoradical states—namely $\mathbf{R3}^{(4+)(\bullet+)}$, $\mathbf{R4}^{(4+)(\bullet+)}$, and $\mathbf{R6}^{(4+)(\bullet+)}$, respectively—in the gas phase. In solution, however, **R4**·6PF_6–**R11**·6PF_6 do not exhibit stabilized monoradical states, owing to solvation effects which stabilize their fully oxidized forms. DFT calculations also reveal that in a vacuum, $\mathbf{R3}^{6+}$ favors its monoradical state to a greater extent than does $\mathbf{R5}^{6+}$ by 10 kcal/mol (Figure 5c), simply because the mechanically interlocked components of $\mathbf{R3}^{6+}$ are forced to reside in closer proximity, resulting in higher Coulombic repulsion. The consequence is that $\mathbf{R3}^{6+}$ is the only one among the nine [2]rotaxanes which exhibits a stabilized monoradical state in solution.

dx.doi.org/10.1021/ja310060n | J. Am. Chem. Soc. 2013, 135, 456–467

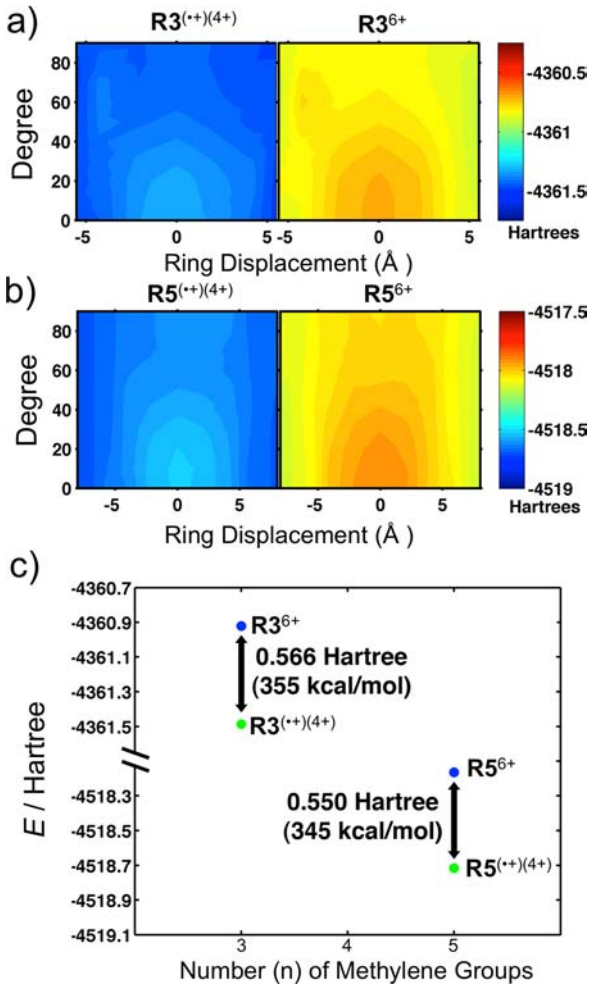

Figure 5. Energy maps for the [2]rotaxanes (a) **R3**·6PF$_6$ and (b) **R5**·6PF$_6$ in their monoradical and fully oxidized states. Zero displacement along the *x* axis represents the co-conformation when the **CBPQT**$^{4+}$ ring resides in the middle of the corresponding dumbbell component. Zero degrees indicates when the long axis of the **CBPQT**$^{4+}$ ring is perpendicular to the plane of the BIPY^{2+} unit. (c) Total energy of two [2]rotaxanes in their fully oxidized forms, **R3**$^{6+}$ and **R5**$^{6+}$ (green dots), and their monoradical forms, **R3**$^{(4+)(\bullet+)}$ and **R5**$^{(4+)(\bullet+)}$ (green dots).

UV/vis/NIR spectroscopy was performed in order to evaluate more deeply the impact of the mechanical bond on the stabilities of the BIPY$^{\bullet+}$ radicals. Zn dust was used to reduce heterogeneously the [2]rotaxane **R3**$^{6+}$ to its trisradical state, namely **R3**$^{3(\bullet+)}$. Upon filtering the excess of Zn dust, the spectrum (Figure 6, purple trace) of **R3**$^{3(\bullet+)}$ exhibits the characteristic feature of BIPY$^{\bullet+}$ radical−radical interactions, i.e., an absorption band (λ_{max} = 523 nm) accompanied by the appearance of a distinctive set of broad NIR bands ($\lambda_{max} \approx$ 875, 1066, and >1600 nm). This observation is in agreement with our previous results obtained for pseudorotaxanes[15] and rotaxanes.[15,17] The broad NIR band centered on 1066 nm can be attributed[33] to an excitation involving all three BIPY$^{\bullet+}$ radical cations. Slowly exposing the solution to air affords us the opportunity to follow the stepwise oxidation of the trisradical **R3**$^{3(\bullet+)}$ to the bisradical **R3**$^{2(\bullet+)(2+)}$ (Figure 6, red trace) and then to the monoradical **R3**$^{(\bullet+)(4+)}$ (Figure 6, blue trace). The absorption band centered on 1066 nm diminishes significantly faster than other bands, indicating this band arises from the

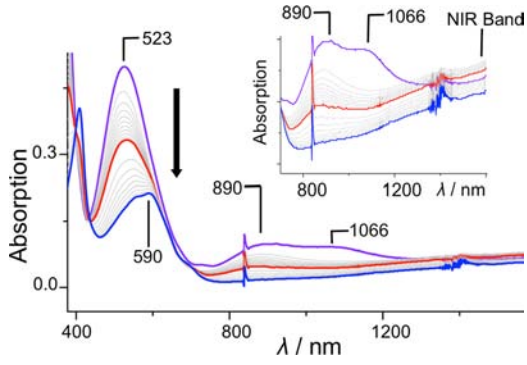

Figure 6. Partial UV/vis absorption spectra of the [2]rotaxane **R3**·6PF$_6$ after it has been reduced with Zn dust and then exposed to air. The spectra were recorded every 2 h in a 2 mm cell-path length cuvette, under the same conditions of temperature (298 K), solvent (MeCN), and concentration (0.25 mM). The purple, red, and blue traces correspond to solutions which have been exposed to air for 0, 20, and 32 h, respectively.

trisradical state. After the solution is exposed to air, the broad NIR band (λ_{max} >1600 nm) undergoes a slight growth before it starts to diminish, an observation which can be explained by the fact that the trisradical trication **R3**$^{3(\bullet+)}$undergoes a one-electron oxidation and is converted into the bisradical tetracation **R3**$^{2(\bullet+)(2+)}$. After the solution is exposed to air for more than 20 h, the absorption band centered on 523 nm begins to undergo a red shift, such that the maximum absorption (λ_{max}) is shifted all the way to 590 nm (Figure 6, blue trace) after a total of 32 h. This observation is attributed to the one-electron oxidation of the **R3**$^{2(\bullet+)(2+)}$ to **R3**$^{(\bullet+)(4+)}$, leading to the formation of an unpaired BIPY$^{\bullet+}$ radical cation which has a characteristic maximum absorption band centered on a longer wavelength than that of a (BIPY$^{\bullet+}$)$_2$ bisradical dication.[34] The red shift of the maximum absorption band is not observed in the spectra (see the SI) of the longer counterparts, namely **R4**$^{6+}$ and **R11**$^{6+}$, an observation which is consistent with the CV studies which demonstrate that the bisradical tetracations in **R4**$^{2(\bullet+)(2+)}$−**R11**$^{2(\bullet+)(2+)}$ undergo simultaneous two-electron oxidations to their fully oxidized states, while **R3**$^{2(\bullet+)(2+)}$ undergoes stepwise oxidation, affording a monoradical state, namely **R3**$^{(\bullet+)(4+)}$.

The oxidations of the shorter rotaxanes from their reduced radical states to their fully oxidized states by atmospheric O_2 are remarkably slower than those observed for the longer ones. For example, the characteristic radical absorption band (see the SI) of the [2]rotaxane **R11**·6PF$_6$ in its reduced state diminishes almost completely after exposure to air for 3 h, while that of **R3**·6PF$_6$ (Figure 6) witnesses a decrease by no more than 70% in its absorption even after 30 h. This observation, together with the electrochemical data, supports the argument that the mechanical bond stabilizes the radical states of the shorter [2]rotaxanes to a much greater extent than in the case of their longer counterparts, by forcing the CBPQT^{4+} rings to reside in closer proximity to the BIPY^{2+} units in the middle of their dumbbells.

The photographs (Figure 7) of the solutions of the reduced [2]rotaxanes **R3**·6PF$_6$−**R9**·6PF$_6$, which were taken at various times after the solutions were exposed to air, provide a direct illustration of the impact of the presence of mechanical bonds on radical stabilization. As expected, upon reduction with Zn dust, all the solutions of the seven [2]rotaxanes turned purple, indicating the formation of trisradical trication states. After

dx.doi.org/10.1021/ja310060n | J. Am. Chem. Soc. 2013, 135, 456−467

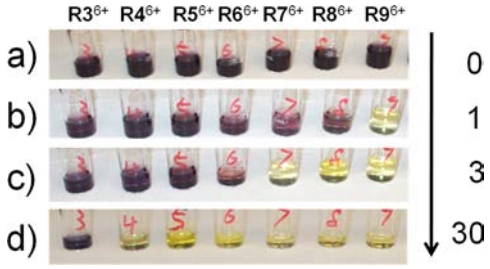

Figure 7. Photographs of 0.25 mM solutions of [2]rotaxanes **R3**·6PF_6–**R9**·6PF_6 in MeCN after they were reduced with Zn dust and then exposed to air for (a) 0 min, (b) 1 h, (c) 3 h, and (d) 30 h.

exposure to air, the purple color of these solutions began to diminish. The solutions of the reduced longer rotaxanes diminished significantly faster than those of the shorter ones. For example, in 1 h, the purple solution of the reduced **R9**·6PF_6 became pale yellow (Figure 7b), indicating that it was converted completely into its fully oxidized state. By contrast, the purple solution of the reduced **R3**·6PF_6 gradually turned to dark blue after exposure to air for 30 h (Figure 7d): it is the characteristic color of $BIPY^{\bullet+}$ radical monomer, an observation supporting the conclusion that the [2]rotaxane $\mathbf{R3}^{6+}$ has a monoradical state.

CONCLUSIONS

A homologous series of [2]rotaxanes comprising $CBPQT^{4+}$ as their ring components, with their dumbbells containing $BIPY^{2+}$ units of varying lengths, have been synthesized using radical templation. We have observed that mechanical bonds, along with the constitution of their dumbbells, can enforce the proximities between the positively charged components in these [2]rotaxanes which (i) stabilize the $BIPY^{\bullet+}$ radical cations of the reduced [2]rotaxanes against oxidation and (ii) influence the activation energy barriers for the $CBPQT^{4+}$ rings shuttling along their dumbbells in the fully oxidized [2]rotaxanes. In agreement with our experimental findings, DFT calculations reveal that the ground states of the rotaxanes become increasingly destabilized while the monoradical states become increasingly more favored as the lengths of the dumbbells become shorter and shorter. We speculate that the stable monoradical states in the shorter rotaxanes brought about by Coulombic repulsion could give rise to through-space mixed valency, whereby one radical electron is delocalized across two or more $BIPY^{2+}$ units. These findings add to our fundamental understanding of the nature of electrostatic barriers and the radical chemistry of molecules containing multiple $BIPY^{2+}$ units. In addition, a new strategy for producing highly stabilized $BIPY^{\bullet+}$ radical cations, resistant to oxidation, has been developed. The strategy opens up opportunities for chemists to use $BIPY^{\bullet+}$ building blocks as stable organic radicals for paramagnetic materials and to develop NEMs for applications in challenging and contemporary arenas, such as conductive molecular electronic devices.

EXPERIMENTAL SECTION

General Methods. All reagents were purchased from commercial suppliers (Aldrich or Fisher) and used without further purification. Thin-layer chromatography (TLC) was performed on silica gel 60 F254 (E. Merck). Column chromatography was carried out on silica gel 60F (Merck 9385, 0.040–0.063 mm). UV/vis spectra were recorded on a Varian 100-Bio spectrophotometer in MeCN or H_2O at room temperature. NMR spectra were recorded on Bruker Avance 600 or Varian P-Inova 500 spectrometers, with working frequencies of 600 and 500 MHz for ^1H nuclei, and 150 and 125 MHz for ^{13}C. Chemical shifts are reported in ppm relative to the signals corresponding to the residual non-deuterated solvents ($CDCl_3$, δ = 7.26 ppm; CD_3CN, δ = 1.94 ppm; CD_3COCD_3, δ = 2.05 ppm). High-resolution mass spectra were measured either on an Applied Biosystems Voyager DE-PRO MALDI TOF mass spectrometer (HR-TOF) or on a Finnigan LCQ iontrap mass spectrometer (HR-ESI). Cyclic voltammetry (CV) experiments were carried out at room temperature in argon-purged solutions in MeCN and H_2O with a Gamry multipurpose instrument (Reference 600) interfaced to a personal computer. CV experiments were performed using a glassy carbon working electrode (0.071 cm^2). The electrode surface was polished routinely with 0.05 μm alumina–water slurry on a felt surface immediately before use. The counter electrode was a Pt coil, and the reference electrode was a saturated calomel electrode. The concentrations of the sample and supporting electrolyte (tetrabutylammonium hexafluorophosphate or tetrabutylammonium chloride) were 1×10^{-3} and 0.1 mol/L, respectively.

Synthesis. General procedures A, B, and C are based in Scheme 2, and general procedure D is based in Scheme 1. Cyclobis(paraquat-*p*-phenylene) tetrakis(hexafluorophosphate)[4c] (**CBPQT**·4PF_6) was prepared according to literature procedures.

Scheme 2. Syntheses of the Tosylates T3–T11 (see General Procedures A and B) and the Viologen Derivatives $V3^{2+}$–$V11^{2+}$ (see General Procedure C)[a]

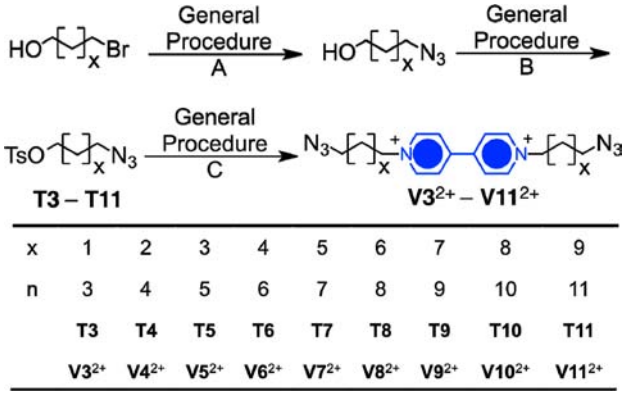

x	1	2	3	4	5	6	7	8	9
n	3	4	5	6	7	8	9	10	11
	T3	**T4**	**T5**	**T6**	**T7**	**T8**	**T9**	**T10**	**T11**
	$V3^{2+}$	$V4^{2+}$	$V5^{2+}$	$V6^{2+}$	$V7^{2+}$	$V8^{2+}$	$V9^{2+}$	$V10^{2+}$	$V11^{2+}$

[a]The PF_6^- counterions are omitted for the sake of clarity.

General Procedure A. The bromo-alcohol (10 mmol) and NaN_3 (1.3 g, 20 mmol) were dissolved in dry DMF (50 mL). The reaction mixture was stirred at 80 °C for 8 h. After cooling to room temperature, the solution was poured into H_2O (200 mL). The resulting mixture was extracted with EtOAc (3 × 20 mL), and the combined organic phases were washed with saturated aqueous NaCl solution (3 × 100 mL). After drying ($MgSO_4$), the solvent was removed in vacuo to afford the corresponding azide as a colorless oil, which was used in the next step without further purification.

General Procedure B. A 50% aqueous NaOH solution (8 mL) was added to a solution of the azide (10 mmol) in THF (50 mL) at 0 °C. After the mixture was stirred for 30 min, TsCl (2.10 g, 11 mmol) in THF (50 mL) was added slowly to the solution. The reaction mixture was stirred for 8 h and then poured into H_2O. The resulting mixture was extracted with $CHCl_3$ (3 × 20 mL), and the combined organic phases were washed with a saturated aqueous NaCl solution (3 × 100 mL). After drying ($MgSO_4$), the solvent was removed under reduced pressure. The residue was purified by column chromatography (SiO_2:hexanes/EtOAc 98:2) to afford the desired tosylate bearing an azide function (**T3**–**T11**).

T3. Following general procedures A and B (based on 1.38 g of 3-bromo-1-propanol), 2.32 g (91% over two steps) of **T3** was isolated (SiO_2:hexanes/EtOAc 98:2) as a light yellow oil. ^1H NMR (500 MHz, $CDCl_3$, 298 K): δ (ppm) = 7.81 (d, J = 8.0 Hz, 2H), 7.38 (d, J = 8.0 Hz, 2H), 4.12 (t, J = 6.0 Hz, 2H), 3.40 (t, J = 6.5 Hz, 2H), 2.47 (s,

dx.doi.org/10.1021/ja310060n | J. Am. Chem. Soc. 2013, 135, 456–467

3H), 1.90 (m, 2H). ^{13}C NMR (125 MHz, $CDCl_3$, 298 K): δ (ppm) = 145.1, 132.6, 130.0, 127.8, 67.2 47.2, 28.3, 21.6.

T4. Following general procedures A and B (based on 1.53 g of 4-bromo-1-butanol), 2.29 g (85% over two steps) of **T4** was isolated (SiO_2:hexanes/EtOAc 98:2) as a light yellow oil. ^{1}H NMR (500 MHz, $CDCl_3$, 298 K): δ (ppm) = 7.81 (d, J = 8.0 Hz, 2H), 7.38 (d, J = 8.0 Hz, 2H), 4.07 (t, J = 6.0 Hz, 2H), 3.30 (t, J = 6.5 Hz, 2H), 2.48 (s, 3H), 1.78−1.62 (m, 4H). ^{13}C NMR (125 MHz, $CDCl_3$, 298 K): δ (ppm) = 145.0, 132.9, 130.0, 127.9, 69.7, 50.7, 26.1, 25.0, 21.7.

T5. Following general procedures A and B (based on 1.67 g of 5-bromo-1-pentanol), 2.44 g (86% over two steps) of **T5** was isolated (SiO_2:hexanes/EtOAc 98:2) as a light yellow oil. ^{1}H NMR (500 MHz, $CDCl_3$, 298 K): δ (ppm) = 7.80 (d, J = 8.5 Hz, 2H), 7.37 (d, J = 8.5 Hz, 2H), 4.04 (t, J = 6.0 Hz, 2H), 3.25 (t, J = 6.5 Hz, 2H), 2.47 (s, 3H), 1.70−1.40 (m, 6H). ^{13}C NMR (125 MHz, $CDCl_3$, 298 K): δ (ppm) = 144.9, 133.0, 129.9, 127.9, 70.2, 51.1, 28.4, 28.2, 22.7, 21.7.

T6. Following general procedures A and B (based on 1.81 g of 6-bromo-1-hexanol), 2.67 g (90% over two steps) of **T6** was isolated (SiO_2:hexanes/EtOAc 98:2) as a light yellow oil. ^{1}H NMR (500 MHz, $CDCl_3$, 298 K): δ (ppm) = 7.75 (d, J = 8.0 Hz, 2H), 7.32 (d, J = 8.0 Hz, 2H), 3.98 (t, J = 6.5 Hz, 2H), 3.19 (t, J = 7.0 Hz, 2H), 2.41 (s, 3H), 1.62−1.28 (m, 8H). ^{13}C NMR (125 MHz, $CDCl_3$, 298 K): δ (ppm) = 144.8, 133.0, 129.9, 127.8, 70.4, 51.2, 28.6, 28.6, 26.0, 24.9, 21.6.

T7. Following general procedures A and B (based on 1.95 g of 7-bromo-1-heptanol), 2.50 g (80% over two steps) of **T7** was isolated (SiO_2:hexanes/EtOAc 98:2) as a light yellow oil. ^{1}H NMR (500 MHz, $CDCl_3$, 298 K): δ (ppm) = 7.80 (d, J = 8.0 Hz, 2H), 7.36 (d, J = 8.0 Hz, 2H), 4.03 (t, J = 6.0 Hz, 2H), 3.25 (t, J = 6.5 Hz, 2H), 2.46 (s, 3H), 1.67−1.28 (m, 10H). ^{13}C NMR (125 MHz, $CDCl_3$, 298 K): δ (ppm) = 144.7, 133.2, 129.8, 127.9, 70.5, 51.4, 28.7, 28.7, 28.4, 26.5, 25.2, 21.6.

T8. Following general procedures A and B (based on 2.09 g of 8-bromo-1-octanol), 2.48 g (76% over two steps) of **T8** was isolated (SiO_2:hexanes/EtOAc 98:2) as a light yellow oil. ^{1}H NMR (500 MHz, $CDCl_3$, 298 K): δ (ppm) = 7.81 (d, J = 8.0 Hz, 2H), 7.37 (d, J = 8.0 Hz, 2H), 4.04 (t, J = 6.0 Hz, 2H), 3.27 (t, J = 6.5 Hz, 2H), 2.47 (s, 3H), 1.67−1.27 (m, 12H). ^{13}C NMR (125 MHz, $CDCl_3$, 298 K): δ (ppm) = 144.7, 133.1, 129.8, 127.9, 70.6, 51.4, 28.9, 28.9, 28.9, 28.8, 26.6, 25.3, 21.7.

T9. Following general procedures A and B (based on 2.23 g of 9-bromo-1-nonanol), 2.27 g (67% over two steps) of **T9** was isolated (SiO_2:hexanes/EtOAc 98:2) as a light yellow oil. ^{1}H NMR (500 MHz, $CDCl_3$, 298 K): δ (ppm) = 7.81 (d, J = 8.0 Hz, 2H), 7.37 (d, J = 8.0 Hz, 2H), 4.04 (t, J = 6.0 Hz, 2H), 3.27 (t, J = 6.5 Hz, 2H), 2.47 (s, 3H), 1.67−1.26 (m, 14H). ^{13}C NMR (125 MHz, $CDCl_3$, 298 K): δ (ppm) = 144.7, 133.2, 129.8, 127.9, 70.7, 51.4, 29.2, 29.0, 28.8, 28.8, 28.8 26.7, 25.3, 21.7.

T10. Following general procedures A and B (based on 2.37 g of 10-bromo-1-decanol), 2.48 g (71% over two steps) of **T10** was isolated (SiO_2:hexanes/EtOAc 98:2) as a light yellow oil. ^{1}H NMR (500 MHz, $CDCl_3$, 298 K): δ (ppm) = 7.80 (d, J = 8.0 Hz, 2H), 7.35 (d, J = 8.0 Hz, 2H), 4.03 (t, J = 6.0 Hz, 2H), 3.26 (t, J = 6.5 Hz, 2H), 2.46 (s, 3H), 1.66−1.24 (m, 16H). ^{13}C NMR (125 MHz, $CDCl_3$, 298 K): δ (ppm) = 144.6, 133.2, 129.8, 127.870.7, 51.5, 29.3, 29.2, 29.1, 28.9, 28.8, 26.6, 25.3, 21.6.

T11. Following general procedures A and B (based on 2.51 g of 11-bromo-1-undecanol), 2.53 g (69% over two steps) of **T11** was isolated (SiO_2:hexanes/EtOAc 98:2) as a light yellow oil. ^{1}H NMR (500 MHz, $CDCl_3$, 298 K): δ (ppm) = 7.75 (d, J = 8.0 Hz, 2H), 7.32 (d, J = 8.0 Hz, 2H), 3.98 (t, J = 6.5 Hz, 2H), 3.22 (t, J = 6.5 Hz, 2H), 2.41 (s, 3H), 1.61−1.54 (m, 4H), 1.32−1.19 (m, 14H). ^{13}C NMR (125 MHz, $CDCl_3$, 298 K): δ (ppm) = 144.7, 133.2, 129.8, 127.8, 70.7, 51.4, 29.4, 29.3, 29.3, 29.1, 28.9, 28.8, 28.7, 26.6, 25.3, 21.6.

General Procedure C. The tosylate (3 mmol) bearing an azide function and 4,4′-bipyridine (156 mg, 1 mmol) were dissolved in MeCN (20 mL). The mixture was stirred at 80 °C for 16 h. The solvent was evaporated, and the residue was purified by column chromatography (SiO_2:MeOH and then 2% NH_4PF_6 in Me_2CO). The fraction in Me_2CO was collected, and the solvent was evaporated under reduced pressure. The resulting residue was washed with H_2O to afford the desired viologen derivatives (**V3**·2PF_6−**V11**·2PF_6) as white powders.

V3·2PF$_6$. Following general procedure C (based on 765 mg of **T3**), 405 mg (66%) of **V3**·2PF_6 was isolated (SiO_2:2% NH_4PF_6 in Me_2CO) as a white power. ^{1}H NMR (500 MHz, CD_3CN, 298 K): δ (ppm) = 8.95 (d, J = 6.0 Hz, 2H), 8.43 (d, J = 6.0 Hz, 2H), 4.73 (t, J = 7.5 Hz, 2H), 3.53 (t, J = 6.5 Hz, 2H), 2.32−2.29 (m, 2H). ^{13}C NMR (125 MHz, CD_3CN, 298 K): δ (ppm) = 149.7, 145.5, 126.9, 59.2, 47.2, 29.5. ESI-HRMS: calcd m/z = 469.1453 $[M - PF_6]^+$, found m/z = 469.1465.

V4·2PF$_6$. Following general procedure C (based on 807 mg of **T4**), 346 mg (54%) of **V4**·2PF_6 was isolated (SiO_2:MeOH and then 2% NH_4PF_6 in Me_2CO) as a white power. ^{1}H NMR (500 MHz, CD_3CN, 298 K): δ (ppm) = 8.93 (d, J = 6.0 Hz, 2H), 8.40 (d, J = 6.0 Hz, 2H), 4.67 (t, J = 7.5 Hz, 2H), 3.44 (t, J = 6.5 Hz, 2H), 2.17−2.08 (m, 2H), 1.71−1.66 (m, 2H). ^{13}C NMR (125 MHz, CD_3CN, 298 K): δ (ppm) = 149.6, 145.3, 126.9, 61.2, 50.0, 28.0, 24.6. ESI-HRMS: calcd m/z = 497.1766 $[M - PF_6]^+$, found m/z = 497.1763.

V5·2PF$_6$. Following general procedure C (based on 847 mg of **T5**), 382 mg (57%) of **V5**·2PF_6 was isolated (SiO_2:MeOH and then 2% NH_4PF_6 in Me_2CO) as a white power. ^{1}H NMR (500 MHz, CD_3CN, 298 K): δ (ppm) = 8.92 (d, J = 5.5 Hz, 2H), 8.40 (d, J = 5.5 Hz, 2H), 4.65 (t, J = 7.5 Hz, 2H), 3.36 (t, J = 6.5 Hz, 2H), 2.08−2.05 (m, 2H), 1.70−1.65 (m, 2H), 1.51−1.45 (m, 2H). ^{13}C NMR (125 MHz, CD_3CN, 298 K): δ (ppm) = 149.6, 145.2, 126.9, 61.5, 50.4, 30.1, 27.4, 22.4. ESI-HRMS: calcd m/z = 525.2088 $[M - PF_6]^+$, found m/z = 525.2074.

V6·2PF$_6$. Following general procedure C (based on 891 mg of **T6**), 314 mg (45%) of **V6**·2PF_6 was isolated (SiO_2:MeOH and then 2% NH_4PF_6 in Me_2CO) as a white power. ^{1}H NMR (500 MHz, CD_3CN, 298 K): δ (ppm) = 8.92 (d, J = 6.5 Hz, 2H), 8.40 (d, J = 5.5 Hz, 2H), 4.64 (t, J = 7.5 Hz, 2H), 3.34 (t, J = 6.5 Hz, 2H), 2.07−2.04 (m, 2H), 1.64−1.59 (m, 2H), 1.47−1.44 (m, 4H). ^{13}C NMR (125 MHz, CD_3CN, 298 K): δ (ppm) = 149.5, 145.2, 126.8, 61.5, 50.5, 30.4, 27.8, 25.3, 24.7. ESI-HRMS: calcd m/z = 553.2392 $[M - PF_6]^+$, found m/z = 553.2385.

V7·2PF$_6$. Following general procedure C (based on 933 mg of **T7**), 413 mg (57%) of **V7**·2PF_6 was isolated (SiO_2:MeOH and then 2% NH_4PF_6 in Me_2CO) as a white power. ^{1}H NMR (500 MHz, CD_3CN, 298 K): δ (ppm) = 8.93 (d, J = 6.0 Hz, 2H), 8.41 (d, J = 5.5 Hz, 2H), 4.65 (t, J = 7.5 Hz, 2H), 3.33 (t, J = 6.5 Hz, 2H), 2.06 (b, 2H), 1.62 (b, 2H), 1.43 (b, 6H). ^{13}C NMR (125 MHz, CD_3CN, 298 K): δ (ppm) = 150.1, 145.7, 127.4, 62.3, 51.2, 31.0, 28.4, 28.2, 26.2, 25.5. ESI-HRMS: calcd m/z = 581.2705 $[M - PF_6]^+$, found m/z = 581.2694.

V8·2PF$_6$. Following general procedure C (based on 975 mg of **T8**), 407 mg (54%) of **V8**·2PF_6 was isolated (SiO_2:MeOH and then 2% NH_4PF_6 in Me_2CO) as a white power. ^{1}H NMR (500 MHz, CD_3CN, 298 K): δ (ppm) = 8.95 (d, J = 6.0 Hz, 2H), 8.43 (d, J = 5.0 Hz, 2H), 4.66 (t, J = 7.5 Hz, 2H), 3.33 (t, J = 6.5 Hz, 2H), 2.06 (b, 2H), 1.62 (b, 2H), 1.54−1.39 (m, 8H). ^{13}C NMR (125 MHz, CD_3CN, 298 K): δ (ppm) = 150.1, 145.8, 127.4, 62.3, 51.3, 31.1, 28.7, 28.6, 28.6, 26.4, 25.6. ESI-HRMS: calcd m/z = 609.3018 $[M - PF_6]^+$, found m/z = 609.3002.

V9·2PF$_6$. Following general procedure C (based on 1.02 g of **T9**), 360 mg (46%) of **V9**·2PF_6 was isolated (SiO_2:MeOH and then 2% NH_4PF_6 in Me_2CO) as a white power. ^{1}H NMR (500 MHz, CD_3CN, 298 K): δ (ppm) = 8.98 (d, J = 5.5 Hz, 2H), 8.46 (d, J = 5.5 Hz, 2H), 4.67 (t, J = 7.5 Hz, 2H), 3.32 (t, J = 6.5 Hz, 2H), 2.06 (b, 2H), 1.62−1.58 (m, 2H), 1.41−1.37 (m, 10H). ^{13}C NMR (125 MHz, CD_3CN, 298 K): δ (ppm) = 150.1, 145.7, 127.4, 62.2, 51.3, 31.1, 29.0, 28.8, 28.6, 28.6, 26.5, 26.7. ESI-HRMS: calcd m/z = 637.3331 $[M - PF_6]^+$, found m/z = 637.3329.

V10·2PF$_6$. Following general procedure C (based on 1.06 g of **T10**), 470 mg (58%) of **V10**·2PF_6 was isolated (SiO_2:MeOH and then 2% NH_4PF_6 in Me_2CO) as a white power. ^{1}H NMR (500 MHz, CD_3CN, 298 K): δ (ppm) = 8.93 (d, J = 6.5 Hz, 2H), 8.42 (d, J = 5.0 Hz, 2H), 4.65 (t, J = 7.5 Hz, 2H), 3.32 (t, J = 6.5 Hz, 2H), 2.06 (b, 2H), 1.63−1.59 (m, 2H), 1.41−1.35 (m, 12H). ^{13}C NMR (125 MHz, CD_3CN, 298 K): δ (ppm) = 150.1, 145.7, 127.4, 62.3, 51.3, 31.1, 29.2, 29.1,

dx.doi.org/10.1021/ja310060n | J. Am. Chem. Soc. 2013, 135, 456−467

28.9, 28.7, 28.6, 26.5, 25.7. ESI-HRMS: calcd m/z = 665.3644 $[M - PF_6]^+$, found m/z = 665.3626.

***V11*·2PF$_6$.** Following general procedure C (based on 1.11 g of **T11**), 561 mg (67%) of **V11**·2PF$_6$ was isolated (SiO_2:MeOH and then 2% NH_4PF_6 in Me_2CO) as a white power. ^{1}H NMR (500 MHz, CD_3CN, 298 K): δ (ppm) = 8.89 (d, J = 6.2 Hz, 2H), 8.37 (d, J = 6.2 Hz, 2H), 4.60 (t, J = 7.5 Hz, 2H), 3.27 (t, J = 7.0 Hz, 2H), 2.02−1.99 (m, 2H), 1.58−1.54 (m, 2H), 1.37−1.30 (m, 14H). ^{13}C NMR (125 MHz, CD_3CN, 298 K): δ (ppm) = 149.5, 145.2, 126.8, 61.8, 50.7, 30.6, 28.8, 28.7, 28.6, 28.5, 28.2, 28.1, 26.0, 25.2. ESI-HRMS: calcd m/z = 693.3957 $[M - PF_6]^+$, found m/z = 693.3952.

Synthesis of the Stopper Precursor ***S***. Acetylenedicarboxylic acid (1.14 g, 10 mmol) and 2,2-dimethyl-1-propanol (8.8 g, 100 mmol) were added to a round-bottomed flask (50 mL). The reaction mixture was heated to 80 °C and stirred for 10 min, after which the solids melted. Concentrated surfuric acid (4 mL) was then added to the flask. The reaction mixture was stirred at 80 °C for 8 h. After cooling to room temperature, the solution was poured into H_2O (200 mL). The resulting mixture was extracted with EtOAc (3 × 20 mL), and the combined organic phases were washed with saturated aqueous NaCl solution (3 × 100 mL). After drying ($MgSO_4$), the solvent was removed in vacuo, and the resulting residue was purified by column chromatography (SiO_2:hexanes/EtOAc 90:10) to afford the desired product **S** (1.83 g, 72%) as a white solid. ^{1}H NMR (500 MHz, $CDCl_3$, 298 K): δ (ppm) = 3.87 (s, 4H), 0.91 (s, 18H). ^{13}C NMR (125 MHz, $CDCl_3$, 298 K): δ (ppm) = 152.1, 76.0, 74.8, 31.4, 26.3.

General Procedure D. As shown in Scheme 1, the appropriate viologen derivative (0.2 mmol) and **CBPQT**·4PF$_6$ (110 mg, 0.1 mmol) were dissolved in MeCN (20 mL). The mixture was purged with Ar while stirring for 30 min, and an excess of zinc dust was added. The reaction mixture turned to purple color after being stirred under an Ar atmosphere for 30 min. The solid was then filtered, and compound **S** was added to the purple filtrate. The reaction mixture was stirred under an Ar atmosphere for 3 days. The solvent was evaporated off, and the residue was purified by column chromatography (SiO_2:MeOH and then 0.1% NH_4PF_6 in Me_2CO). Yellow fractions were collected and concentrated to a minimum volume, from which the products were precipitated on addition of H_2O, before being collected by filtration to afford the [2]rotaxanes (**R3**·6PF$_6$−**R11**·6PF$_6$) as white powders.

***R3*·6PF$_6$.** Following general procedure D (based on 122 mg of **V3**·2PF$_6$), 11 mg (5%) of **R3**·6PF$_6$ was isolated (SiO_2:MeOH and then 2% NH_4PF_6 in Me_2CO) as a white power. ^{1}H NMR (600 MHz, CD_3CN, 343K): δ (ppm) = 9.04 (d, J = 6.6 Hz, 4H), 8.95 (d, J = 6.0 Hz, 8H), 8.63 (d, J = 6.6 Hz, 4H), 8.12 (d, J = 6.0 Hz, 8H), 7.77 (s, 8H), 5.88 (s, 8H), 4.56 (t, J = 8.4 Hz, 4H), 4.29 (s, 4H), 4.07 (s, 4H), 3.10 (b, 4H), 2.27 (br, 2H), 1.86 (br, 4H), 1.19 (s, 18H), 1.13 (s, 18H). ^{13}C NMR (125 MHz, CD_3COCD_3, 298 K): δ (ppm) = 160.6, 157.2, 150.4, 146.3, 146.1, 146.0, 141.1, 136.1, 130.9, 127.3, 125.6, 116.6, 65.5, 65.0, 59.0, 47.2, 31.2, 31.1, 25.9, 25.5, −0.0. ESI-HRMS: calcd m/z = 966.3007 $[M - 2PF_6]^{2+}$, found m/z = 966.2987.

***R4*·6PF$_6$.** Following general procedure D (based on 128 mg of **V4**·2PF$_6$), 15 mg (7%) of **R4**·6PF$_6$ was isolated (SiO_2:MeOH and then 2% NH_4PF_6 in Me_2CO) as a white power. ^{1}H NMR (600 MHz, CD_3COCD_3, 233 K): δ (ppm) = 9.63 (br, 4H), 9.55 (br, 2H), 9.32 (br, 2H), 9.27 (br, 4H), 8.89 (d, J = 6.6 Hz, 4H), 8.87 (br, 4H), 8.35 (br, 4H), 7.95 (s, 8H), 6.09 (s, 8H), 5.06 (br, 4H), 4.77 (br, 2H), 4.49 (s, 2H), 4.16 (s, 2H), 4.06 (s, 2H), 4.05 (s, 2H), 2.28 (br, 2H), 2.17 (br, 2H), 2.13 (br, 2H), 1.57 (br, 2H), 1.44 (br, 4H), 1.24 (s, 9H), 1.13 (s, 9H), 0.98 (s, 9H), 0.97 (s, 9H), −0.44 (br, 2H), −0.60 (br, 2H), −1.90 (br, 2H). ^{13}C NMR (125 MHz, CD_3CN, 298 K): δ (ppm) = 160.6, 150.2, 146.6, 145.9, 145.7, 135.8, 130.7, 127.3, 125.7, 116.6, 65.3, 60.8, 49.4, 31.2, 31.1, 25.5, −0.0. ESI-HRMS: calcd m/z = 2105.5969 $[M - PF_6]^+$, found m/z = 2105.5978.

***R5*·6PF$_6$.** Following general procedure D (based on 134 mg of **V5**·2PF$_6$), 70 mg (31%) of **R5**·6PF$_6$ was isolated (SiO_2:MeOH and then 2% NH_4PF_6 in Me_2CO) as a white power. ^{1}H NMR (600 MHz, CD_3COCD_3, 233 K): δ (ppm) = 9.58 (br, 6H), 9.46 (br, 4H), 9.30 (br, 2H), 8.93 (d, J = 6.6 Hz, 4H), 8.82 (br, 4H), 8.55 (br, 4H), 7.88 (s, 8H), 6.14 (s, 8H), 5.03 (br, 2H), 4.80 (br, 2H), 4.66 (br, 2H), 4.34 (s, 2H), 4.28 (s, 2H), 4.07 (s, 4H), 2.28 (br, 2H), 2.01 (br, 2H), 1.84 (br, 2H), 1.71 (br, 2H), 1.53 (br, 2H), 1.16 (s, 9H), 1.10 (s, 9H), 0.97 (br, 18H), 0.28 (br, 4H). ^{13}C NMR (125 MHz, CD_3CN, 298 K): δ (ppm) = 161.6, 151.2, 148.4, 147.1, 146.9, 137.0, 131.8, 128.3, 127.2, 66.2, 62.6, 50.6, 32.3, 32.2, 31.7, 26.9, 26.7. ESI-HRMS: calcd m/z = 2133.6265 $[M - PF_6]^+$, found m/z = 2133.6398.

***R6*·6PF$_6$.** Following general procedure D (based on 140 mg of **V6**·2PF$_6$), 23 mg (10%) of **R6**·6PF$_6$ was isolated (SiO_2:MeOH and then 2% NH_4PF_6 in Me_2CO) as a white power. ^{1}H NMR (600 MHz, CD_3COCD_3, 233 K): δ (ppm) = 9.78 (d, J = 6.6 Hz, 4H), 9.54 (d, J = 6.0 Hz, 2H), 9.43 (d, J = 6.6 Hz, 4H), 9.35 (d, J = 6.0 Hz, 2H), 9.13 (d, J = 5.4 Hz, 4H), 8.90 (d, J = 5.4 Hz, 4H), 8.84 (d, J = 6.6 Hz, 4H), 7.70 (s, 8H), 6.16 (d, J = 13.8 Hz, 4H), 6.05 (d, J = 13.8 Hz, 4H), 5.00 (t, J = 7.2 Hz, 2H), 4.71 (t, J = 7.2 Hz, 2H), 4.65 (t, J = 6.0 Hz, 2H), 4.35 (s, 2H), 4.19 (s, 2H), 4.07 (s, 2H), 4.04 (s, 2H), 2.87 (br, 2H), 2.21 (br, 2H), 1.92 (br, 2H), 1.52 (br, 2H), 1.41 (br, 4H), 1.07 (s, 9H), 1.04 (s, 9H), 0.98 (s, 9H), 0.97 (s, 9H). ^{13}C NMR (125 MHz, CD_3COCD_3, 298 K): δ (ppm) = 160.3, 158.4, 150.1, 148.3, 146.0, 145.6 136.1, 130.4, 127.3, 127.2, 65.0, 64.7, 53.9, 31.1, 31.0, 25.6, 25.5, 25.2, 0.0. ESI-HRMS: calcd m/z = 2161.6595 $[M - PF_6]^+$, found m/z = 2161.6571, and calcd m/z = 1008.3476 $[M - 2PF_6]^{2+}$, found m/z = 1008.3456.

***R7*·6PF$_6$.** Following general procedure D (based on 146 mg of **V7**·2PF$_6$), 58 mg (25%) of **R7**·6PF$_6$ was isolated (SiO_2:MeOH and then 2% NH_4PF_6 in Me_2CO) as a white power. ^{1}H NMR (600 MHz, CD_3COCD_3, 233 K): δ (ppm) = 9.79 (d, J = 6.0 Hz, 4H), 9.55 (d, J = 6.6 Hz, 6H), 9.26 (d, J = 6.0 Hz, 2H), 9.19 (d, J = 6.0 Hz, 4H), 8.91 (d, J = 4.8 Hz, 6H), 8.88 (d, J = 6.6 Hz, 2H), 7.79 (s, 8H), 6.17 (d, J = 13.6 Hz, 4H), 6.06 (d, J = 13.7 Hz, 4H), 5.00 (t, J = 7.2 Hz, 2H), 4.78 (br, 2H), 4.64 (t, J = 6.6 Hz, 2H), 4.32 (s, 2H), 4.20 (s, 2H), 4.07 (s, 2H), 4.03 (s, 2H), 3.25 (br, 2H), 2.19 (br, 2H), 1.89 (br, 2H), 1.68 (br, 2H), 1.43 (br, 4H), 1.30 (br, 2H), 1.08 (s, 9H), 1.03 (s, 9H), 0.97 (s, 18H), 0.25 (br, 2H), −0.29 (br, 2H), −1.59 (br, 2H), −1.86 (br, 2H). ^{13}C NMR (125 MHz, CD_3COCD_3, 298 K): δ (ppm) = 160.3, 158.4, 150.1, 148.3, 146.0, 145.6 136.1, 130.4, 127.3, 127.2, 65.0, 64.7, 53.9, 31.1, 31.0, 25.6, 25.5, 25.2, −0.0. ESI-HRMS: calcd m/z = 1022.3632 $[M - PF_6]^+$, found m/z = 1022.3640.

***R8*·6PF$_6$.** Following general procedure D (based on 152 mg of **V8**·2PF$_6$), 64 mg (27%) of **R8**·6PF$_6$ was isolated (SiO_2:MeOH and then 2% NH_4PF_6 in Me_2CO) as a white power. ^{1}H NMR (600 MHz, CD_3COCD_3, 233 K): δ (ppm) = 9.79 (d, J = 6.0 Hz, 4H), 9.61 (d, J = 6.0 Hz, 4H), 9.56 (d, J = 7.2 Hz, 2H), 9.22 (d, J = 6.6 Hz, 2H), 9.17 (d, J = 4.8 Hz, 4H), 8.96 (d, J = 6.6 Hz, 2H), 8.91 (br, 6H), 7.86 (s, 8H), 6.18 (d, J = 13.8 Hz, 4H), 6.10 (d, J = 13.8 Hz, 4H), 4.99 (t, J = 7.2 Hz, 2H), 4.82 (br, 2H), 4.63 (t, J = 7.2 Hz, 2H), 4.30 (s, 2H), 4.19 (s, 2H), 4.08 (s, 2H), 4.04 (s, 2H), 3.71 (br, 2H), 2.19 (br, 2H), 1.89 (br, 4H), 1.44−1.18 (m, 8H), 1.07 (s, 9H), 1.03 (s, 9H), 0.98 (s, 18H), 0.46 (br, 2H), 0.28 (br, 2H), −0.70 (br, 2H), −1.64 (br, 2H), −1.85 (br, 2H). ^{13}C NMR (125 MHz, CD_3COCD_3, 298 K): δ (ppm) = 151.1, 149.3, 147.1, 146.5 137.4, 131.5, 128.3, 128.1, 77.3, 76.6, 75.7, 65.8, 63.1, 62.6, 51.0, 50.4, 32.1, 26.9, 26.7. ESI-HRMS: calcd m/z = 1036.3789 $[M - 2PF_6]^{2+}$, found m/z = 1036.3796.

***R9*·6PF$_6$.** Following general procedure D (based on 157 mg of **V9**·2PF$_6$), 67 mg (28%) of **R9**·6PF$_6$ was isolated (SiO_2:MeOH and then 2% NH_4PF_6 in Me_2CO) as a white power. ^{1}H NMR (600 MHz, CD_3COCD_3, 233 K): δ (ppm) = 9.79 (br, 4H), 9.61 (br, 4H), 9.56 (d, J = 6.6 Hz, 2H), 9.23 (d, J = 6.6 Hz, 2H), 9.14 (br, 4H), 8.94 (d, J = 6.6 Hz, 2H), 8.91 (br, 6H), 7.88 (s, 8H), 6.17 (d, J = 13.2 Hz, 4H), 6.10 (d, J = 13.2 Hz, 4H), 4.99 (t, J = 7.2 Hz, 2H), 4.84 (br, 2H), 4.63 (t, J = 7.2 Hz, 2H), 4.26 (s, 2H), 4.17 (s, 2H), 4.08 (s, 2H), 4.05(br, 2H), 4.03 (s, 2H), 2.19 (br, 2H), 1.99 (br, 2H), 1.88 (br, 2H), 1.44 (br, 2H), 1.35 (br, 2H), 1.29 (br, 4H), 1.05 (s, 9H), 1.02 (s, 9H), 0.98 (s, 18H), 0.82 (br, 4H), −0.42 (br, 2H), −0.96 (br, 2H), −1.33 (br, 2H), −1.76 (br, 2H). ^{13}C NMR (125 MHz, CD_3COCD_3, 298 K): δ (ppm) = 160.3, 160.0, 151.1, 149.3, 147.1, 146.9, 146.5, 137.4, 131.5, 130.7, 130.4, 128.3, 128.0, 77.2, 76.6, 75.6, 75.1, 66.1, 65.8, 63.2, 62.8, 51.1, 50.6, 32.4, 32.2, 32.1, 27.5, 27.1, 27.0, 26.7, 15.6. ESI-HRMS: calcd m/z = 1050.3946 $[M - 2PF_6]^{2+}$, found m/z = 1050.3970.

***R10*·6PF$_6$.** Following general procedure D (based on 162 mg of **V10**·2PF$_6$), 51 mg (21%) of **R10**·6PF$_6$ was isolated (SiO_2:MeOH and

dx.doi.org/10.1021/ja310060n | J. Am. Chem. Soc. 2013, 135, 456−467

then 2% NH_4PF_6 in Me_2CO) as a white power. ^{1}H NMR (600 MHz, CD_3COCD_3, 233 K): δ (ppm) = 9.79 (br, 4H), 9.63 (br, 4H), 9.56 (d, J = 6.6 Hz, 2H), 9.25 (d, J = 6.0 Hz, 2H), 9.11 (br, 4H), 8.94 (b, 8H), 7.90 (s, 8H), 6.17 (d, J = 13.8 Hz, 4H), 6.10 (d, J = 13.8 Hz, 4H), 4.99 (t, J = 7.2 Hz, 2H), 4.86 (br, 2H), 4.63 (t, J = 7.2 Hz, 2H), 4.31(br, 2H), 4.23 (s, 2H), 4.14 (s, 2H), 4.07 (s, 2H), 4.03 (s, 2H), 2.19 (br, 2H), 1.88 (br, 2H), 1.44 (br, 2H), 1.35 (br, 2H), 1.27 (br, 8H), 1.17 (br, 2H), 1.03 (s, 9H), 1.02 (s, 9H), 0.98 (s, 18H), 0.05 (br, 4H), −0.35 (br, 2H), −1.07 (br, 2H), −1.15 (br, 2H), −1.56 (br, 2H). ^{13}C NMR (125 MHz, CD_3COCD_3, 298 K): δ (ppm) = 161.5, 161.3, 160.0, 159.6, 151.1, 149.3, 147.1, 137.4, 131.5, 130.8, 128.3, 128.0, 77.1, 76.6, 75.5, 75.1, 66.1, 65.9, 63.2, 63.0, 51.1, 50.7, 32.2, 32.1, 27.4, 27.2, 27.0, 26.7, 15.6. ESI-HRMS: calcd m/z = 1064.4102 $[M - 2PF_6]^{2+}$, found m/z = 1064.4145.

***R11*·6PF$_6$.** Following general procedure D (based on 168 mg of **V11**·2PF$_6$), 68 mg (28%) of **R11**·6PF$_6$ was isolated (SiO_2:MeOH and then 2% NH_4PF_6 in Me_2CO) as a white power. ^{1}H NMR (600 MHz, CD_3COCD_3, 233 K): δ (ppm) = 9.78 (d, J = 6.6 Hz, 4H), 9.64 (d, J = 6.6 Hz, 4H), 9.54 (d, J = 7.2 Hz, 2H), 9.28 (d, J = 6.6 Hz, 2H), 9.09 (d, J = 6.6 Hz, 4H), 8.94−8.90 (m, 8H), 7.92 (s, 8H), 6.15 (d, J = 13.8 Hz, 4H), 6.10 (d, J = 13.8 Hz, 4H), 4.98 (t, J = 7.2 Hz, 2H), 4.88 (t, J = 7.8 Hz, 2H), 4.63 (t, J = 7.2 Hz, 2H), 4.45(t, J = 7.8 Hz, 2H), 4.21 (s, 2H), 4.13 (s, 2H), 4.08 (s, 2H), 4.03 (s, 2H), 2.18 (br, 2H), 1.88 (br, 2H), 2.13 (br, 2H), 1.88 (br, 2H), 1.44 (br, 2H), 1.35 (br, 2H), 1.27−1.24 (br, 10H), 1.07 (br, 2H), 1.03 (s, 9H), 1.02 (s, 9H), 0.98 (s, 9H), 0.97(s, 9H), 0.26 (br, 2H), 0.06 (br, 2H), −0.61 (br, 4H), −1.21 (br, 2H), −1.41 (br, 2H). ^{13}C NMR (125 MHz, CD_3COCD_3, 298 K): δ (ppm) = 160.3, 160.2, 158.7, 158.5, 150.0, 145.9, 145.8, 145.4, 140.0, 139.7, 136.3, 130.3, 129.7, 129.6, 127.1, 126.9, 116.6, 75.9, 75.4, 74.3, 74.0, 64.7, 62.0, 61.9, 50.0, 49.7, 48.7, 31.3, 31.1, 30.9, 26.2, 26.0, 25.9, 25.6, 25.5, −0.0. ESI-HRMS: calcd m/z = 1078.4259 $[M - 2PF_6]^{2+}$, found m/z = 1078.4262.

Computational Methods. All DFT calculations were performed with the Q-Chem 4.0 software package.[35] Initial geometry optimizations were performed on all systems using the Universal Force Field (UFF), followed by quantum optimization at the B3LYP/6-31G* level of theory. The geometries of the ring and dumbbell components were optimized separately in a vacuum. For the interaction energy calculations the optimized ring and dumbbell components were brought together and the M06-2X functional was employed with the 6-31G* basis set to more accurately treat the dispersion interactions of these compounds. A systematic protocol was used for the placement of the ring on the dumbbell component in order to sample accurately the translational and rotational degrees of freedom for the ring along the dumbbell component. This protocol consisted of placing the ring along the dumbbell at sites chosen to sample the translational space. Rotation of the ring relative to the dumbbell component was also carried out at each of these sites. Ring and dumbbell internal geometries were held fixed during this process; only translation and rotation of the ring component were considered. The interaction energy was calculated as the difference in energy between the threaded system at a given geometry and the separated components. No correction was made for the basis set superposition error.

■ ASSOCIATED CONTENT

Supporting Information

Full details of instrumentation and analytical techniques; synthesis and characterization data for the [2]rotaxane **R3**·6PF$_6$−**R11**·6PF$_6$ and their precursors; ^{1}H−^{1}H COSY and variable-temperature ^{1}H NMR spectroscopic investigation of the [2]rotaxane **R3**·6PF$_6$−**R11**·6PF$_6$; UV/vis absorption spectra of **R4**·6PF$_6$ and **R11**·6PF$_6$ after reduction followed by exposure to air; cyclic voltammograms of **R3**·6PF$_6$−**R11**·6PF$_6$; high-resolution mass spectra of the [2]rotaxane **R3**·6PF$_6$ and its corresponding dumbbell **D3**·2PF$_6$, as well as the [2]rotaxanes **R4**·6PF$_6$ and **R6**·6PF$_6$; ^{1}H NMR spectroscopic investigation on the dethreading of **R′3**·6PF$_6$; quantum chemical investigation by means of DFT calculations. This material is available free of charge via the Internet at http://pubs.acs.org.

■ AUTHOR INFORMATION

Corresponding Author

stoddart@northwestern.edu

Notes

The authors declare no competing financial interest.

■ ACKNOWLEDGMENTS

This work was supported by the Non-Equilibrium Energy Center (NERC), which is an Energy Frontier Research Center funded by the U.S. Department of Energy, Office of Science, Office of Basic Energy Sciences award DE-SC0000989, and by the NSF MRSEC program (grant DMR-1121262) at the Materials Research Center of Northwestern University. A.C.F. acknowledges support from an NSF Graduate Research Fellowship. J.C.B. acknowledges support from a DoD National Defense Science and Engineering Graduate Fellowship and a Ryan Fellowship. C.K. thanks the Royal Society in the UK for support as a Newton Fellow Alumnus.

■ REFERENCES

(1) (a) Lehn, J.-M. *Angew. Chem., Int. Ed. Engl.* **1990**, *29*, 1304. (b) Lehn, J.-M. *Science* **1993**, *260*, 1762. (c) Lehn, J.-M. *Supramolecular Chemistry: Concepts and Perspectives*; Wiley VCH: Weinheim, Germany, 1995. (d) Beer, P. D.; Gale, P. A.; Smith, D. K. *Supramolecular Chemistry*; Oxford University Press: Oxford, UK, 1999. (e) Steed, J. W.; Atwood, J. L. *Supramolecular Chemistry*; Wiley VCH: Weinheim, Germany, 2009. (f) Dodziuk, H. *Introduction to Supramolecular Chemistry*; Kluwer: Dordrecht, 2002. (g) Stoddart, J. F. *Nat. Chem.* **2009**, *1*, 14.

(2) Olson, M. A.; Botros, Y. Y.; Stoddart, J. F. *Pure Appl. Chem.* **2010**, *82*, 1569.

(3) (a) Monk, P. M. S. *The Viologens: Physicochemical Properties, Synthesis and Applications of the Salts of 4,4′-Bipyridine*; Wiley-VCH: Weinheim, 1998. (b) Monk, P. M. S.; Hodgkinson, N. M.; Partridge, R. D. *Dyes Pigm.* **1999**, *43*, 241.

(4) (a) Odell, B.; Reddington, M. V.; Slawin, A. M. Z.; Spencer, N.; Stoddart, J. F.; Williams, D. J. *Angew. Chem., Int. Ed. Engl.* **1988**, *27*, 1547. (b) Brown, C. L.; Philp, D.; Stoddart, J. F. *Synlett* **1991**, 462. (c) Asakawa, M.; Dehaen, W.; L'abbé, G.; Menzer, S.; Nouwen, J.; Raymo, F. M.; Stoddart, J. F.; Williams, D. J. *J. Org. Chem.* **1996**, *61*, 9591. (d) Sue, C.-H.; Basu, S.; Fahrenbach, A. C.; Shveyd, A. K.; Dey, S. K.; Botros, Y. Y.; Stoddart, J. F. *Chem. Sci.* **2010**, *1*, 119.

(5) (a) Schill, G. *Catenanes, Rotaxanes and Knots*; Academic Press: New York, 1971. (b) Amabilino, D. B.; Stoddart, J. F. *Chem. Rev.* **1995**, *95*, 2725. (c) Sauvage, J.-P.; Dietrich-Buchecker, C. O. *Molecular Catenanes, Rotaxanes and Knots: A Journey Through the World of Molecular Topology*; John Wiley and Sons: New York, 1999. (d) Champin, B.; Mobian, P.; Sauvage, J.-P. *Chem. Soc. Rev.* **2007**, *36*, 358. (e) Stoddart, J. F.; Colquhoun, H. M. *Tetrahedron* **2008**, *64*, 8231. (f) Rijs, A. M.; Compagnon, I.; Oomens, J.; Hannam, J. S.; Leigh, D. A.; Buma, W. J. *J. Am. Chem. Soc.* **2009**, *131*, 2428. (g) Crowley, J. D.; Goldup, S. M.; Lee, A.-L.; Leigh, D. A.; McBurney, R. T. *Chem. Soc. Rev.* **2009**, *38*, 1530. (h) Mateo-Alonso, A. *Chem. Commun.* **2010**, 9089. (i) Beves, J. E.; Blight, B. A.; Campbell, C. J.; Leigh, D. A.; McBurney, R. T. *Angew. Chem., Int. Ed.* **2011**, *50*, 9260.

(6) (a) Livoreil, A.; Dietrich-Buchecker, C. O.; Sauvage, J.-P. *J. Am. Chem. Soc.* **1994**, *116*, 9399. (b) Asakawa, M.; Ashton, P. R.; Balzani, V.; Credi, A.; Hamers, C.; Mattersteig, G.; Montalti, M.; Shipway, A. N.; Spencer, N.; Stoddart, J. F.; Tolley, M. S.; Venturi, M.; White, A. J. P.; Williams, D. J. *Angew. Chem., Int. Ed.* **1998**, *37*, 333. (c) Cao, D.; Amelia, M.; Klivansky, L. M.; Koshkakaryan, G.; Khan, S. I.; Semeraro, M.; Silvi, S.; Venturi, M.; Credi, A.; Liu, Y. *J. Am. Chem. Soc.* **2010**, *132*, 1110. (d) Evans, N. H.; Serpell, C. J.; Beer, P. D. *Angew. Chem., Int. Ed.*

2011, *50*, 2507. (e) Yang, W.; Li, Y.; Zhang, J.; Chen, N.; Chen, S.; Liu, H.; Li, Y. *J. Org. Chem.* **2011**, *76*, 7750. (f) Cougnon, F. B. L.; Au-Yeung, H. Y.; Pantos, G. D.; Sanders, J. K. M. *J. Am. Chem. Soc.* **2011**, *133*, 3198. (g) Zhu, Z.; Fahrenbach, A. C.; Li, H.; Barnes, J. C.; Liu, Z.; Dyar, S. M.; Zhang, H.; Lei, J.; Carmieli, R.; Sarjeant, A. A.; Stern, C. L.; Wasielewski, M. R.; Stoddart, J. F. *J. Am. Chem. Soc.* **2012**, *134*, 11709.

(7) (a) Qu, D.-H.; Wang, Q.-C.; Tian, H. *Angew. Chem., Int. Ed.* **2005**, *44*, 5296. (b) Zheng, H.; Zhou, W.; Lv, J.; Yin, X.; Li, Y.; Liu, H.; Li, Y. *Chem. Eur. J.* **2009**, *15*, 13253. (c) Jiang, Q.; Zhang, H.-Y.; Han, M.; Ding, Z.-J.; Liu, Y. *Org. Lett.* **2010**, *12*, 1728. (d) Romuald, C.; Busseron, E.; Coutrot, F. *J. Org. Chem.* **2010**, *75*, 6516. (e) Jiang, Y.; Guo, J.-B.; Chen, C.-F. *Org. Lett.* **2010**, *12*, 4248. (f) Olsen, J.-C.; Fahrenbach, A. C.; Trabolsi, A.; Friedman, D. C.; Dey, S. K.; Gothard, C. M.; Shveyd, A. K.; Gasa, T. B.; Spruell, J. M.; Olson, M. A.; Wang, C.; Jacquot de Rouville, H.-P.; Botros, Y. Y.; Stoddart, J. F. *Org. Biomol. Chem.* **2011**, *9*, 7126. (g) Dey, S. K.; Coskun, A.; Fahrenbach, A. C.; Barin, G.; Basuray, A. N.; Trabolsi, A.; Botros, Y. Y.; Stoddart, J. F. *Chem. Sci.* **2011**, *2*, 1046. (h) Yang, W.; Li, Y.; Liu, H.; Chi, L.; Li, Y. *Small* **2012**, *8*, 504. (i) Barnes, J. C.; Fahrenbach, A. C.; Dyar, S. M.; Frasconi, M.; Giesener, M. A.; Zhu, Z.; Liu, Z.; Hartlieb, K. J.; Carmieli, R.; Wasielewski, M. R.; Stoddart, J. F. *Proc. Natl. Acad. Sci. U.S.A.* **2012**, *109*, 11446.

(8) (a) Ashton, P. R.; Odell, B.; Reddington, M. V.; Slawin, A. M. Z.; Stoddart, J. F.; Williams, D. J. *Angew. Chem., Int. Ed. Engl.* **1988**, *27*, 1550. (b) Hunter, C. A.; Sanders, J. K. M. *J. Am. Chem. Soc.* **1990**, *112*, 5525. (c) Amabilino, D. B.; Ashton, P. R.; Reder, A. S.; Spencer, N.; Stoddart, J. F. *Angew. Chem., Int. Ed. Engl.* **1994**, *33*, 1286. (d) Ashton, P. R.; Ballardini, R.; Balzani, V.; Credi, A.; Gandolfi, M. T.; Menzer, S.; Pérez-García, L.; Prodi, L.; Stoddart, J. F.; Venturi, M.; White, A. J. P.; Williams, D. J. *J. Am. Chem. Soc.* **1995**, *117*, 11171. (e) Coumans, R. G. E.; Elemans, J. A. A. W.; Thordarson, P.; Nolte, R. J. M.; Rowan, A. E. *Angew. Chem., Int. Ed.* **2003**, *42*, 650. (f) Barin, G.; Coskun, A.; Fouda, M. M. G.; Stoddart, J. F. *ChemPlusChem* **2012**, *77*, 159.

(9) (a) Bryce, M. R. *J. Mater. Chem.* **2000**, *10*, 589. (b) Nielsen, M. B.; Lomholt, C.; Becher, J. *Chem. Soc. Rev.* **2000**, *29*, 153. (c) Segura, J. L.; Martín, N. *Angew. Chem., Int. Ed.* **2001**, *40*, 1372. (d) Inagi, S.; Naka, K.; Chujo, Y. *J. Mater. Chem.* **2007**, *17*, 4122. (e) Martin, N.; Sánchez, L.; Herranz, M. Á.; Illescas, B.; Guldi, D. M. *Acc. Chem. Res.* **2007**, *40*, 1015. (f) Canevet, D.; Sallé, M.; Zhang, G. X.; Zhang, D. Q.; Zhu, D. B. *Chem. Commun.* **2009**, 2245.

(10) (a) Ashton, P. R.; Chrystal, E. J. T.; Mathias, J. P.; Parry, K. P.; Slawin, A. M. Z.; Spencer, N.; Stoddart, J. F.; Williams, D. J. *Tetrahedron Lett.* **1987**, *28*, 6367. (b) Amabilino, D. B.; Ashton, P. R.; Balzani, V.; Boyd, S. E.; Credi, A.; Lee, J. Y.; Menzer, S.; Stoddart, J. F.; Venturi, M.; Williams, D. J. *J. Am. Chem. Soc.* **1998**, *120*, 4295. (c) Bruns, C. J.; Basu, S.; Stoddart, J. F. *Tetrahedron Lett.* **2010**, *51*, 983.

(11) (a) Houk, K. N.; Menzer, S.; Newton, S. P.; Raymo, F. M.; Stoddart, J. F.; Williams, D. J. *J. Am. Chem. Soc.* **1999**, *121*, 1479. (b) Raymo, F. M.; Bartberger, M. D.; Houk, K. N.; Stoddart, J. F. *J. Am. Chem. Soc.* **2001**, *123*, 9264.

(12) (a) Kosower, E. M.; Cotter, J. L. *J. Am. Chem. Soc.* **1964**, *86*, 5524. (b) Bruinink, J.; Kregting, C. G. A.; Ponjeé, J. J. *J. Electrochem. Soc.* **1977**, *124*, 1854. (c) Bruinink, J.; Kregting, C. G. A. *J. Electrochem. Soc.* **1978**, *125*, 1397. (d) Adar, E.; Degani, Y.; Goren, Z.; Willner, I. *J. Am. Chem. Soc.* **1986**, *108*, 4696. (e) Yasuda, A.; Mori, H.; Seto, J. *J. Appl. Electrochem.* **1987**, *17*, 567.

(13) (a) Yoshizawa, M.; Kumazawa, K.; Fujita, M. *J. Am. Chem. Soc.* **2005**, *127*, 13456. (b) Spruell, J. M.; Coskun, A.; Friedman, D. C.; Forgan, R. S.; Sarjeant, A. A.; Trabolsi, A.; Fahrenbach, A. C.; Barin, G.; Paxton, W. F.; Dey, S. K.; Olson, M. A.; Benítez, D.; Tkatchouk, E.; Colvin, M. T.; Carmielli, R.; Caldwell, S. T.; Rosair, G. M.; Hewage, S. G.; Duclairoir, F.; Seymour, J. L.; Slawin, A. M. Z.; Goddard, W. A., III; Wasielewski, M. R.; Cooke, G.; Stoddart, J. F. *Nature Chem.* **2010**, *2*, 870. (c) Coskun, A.; Spruell, J. M.; Barin, G.; Fahrenbach, A. C.; Forgan, R. S.; Colvin, M. T.; Carmielli, R.; Benítez, D.; Tkatchouk, E.; Friedman, D. C.; Sarjeant, A. A.; Wasielewski, M. R.; Goddard, W. A., III; Stoddart, J. F. *J. Am. Chem. Soc.* **2011**, *133*, 4538.

(14) Jeon, W. S.; Ziganshina, A. Y.; Lee, J. W.; Ko, Y. H.; Kang, J.-K.; Lee, C.; Kim, K. *Angew. Chem., Int. Ed.* **2003**, *42*, 4097.

(15) (a) Trabolsi, A.; Khashab, N.; Fahrenbach, A. C.; Friedman, D. C.; Colvin, M. T.; Cotí, K. K.; Benítez, D.; Tkatchouk, E.; Olsen, J.-C.; Belowich, M. E.; Carmielli, R.; Khatib, H. A.; Goddard, W. A., III; Wasielewski, M. R.; Stoddart, J. F. *Nature Chem.* **2010**, *2*, 42. (b) Fahrenbach, A. C.; Barnes, J. C.; Lanfranchi, D. A.; Li, H.; Coskun, A.; Gassensmith, J. J.; Liu, Z.; Benítez, D.; Trabolsi, A.; Elhabiri, M.; Stoddart, J. F. *J. Am. Chem. Soc.* **2012**, *134*, 3061. (c) Fahrenbach, A. C.; Zhu, Z.; Cao, D.; Liu, W.-G.; Li, H.; Dey, S. K.; Basu, S.; Trabolsi, A.; Botros, Y. Y.; Goddard, W. A., III; Stoddart, J. F. *J. Am. Chem. Soc.* **2012**, *134*, 16275.

(16) The argument that the preorganized cavity of a $CBPQT^{2(\bullet+)}$ ring can stabilize the $(BIPY^{\bullet+})_2$ radical dimers in a $BIPY^{\bullet+}\subset CBPQT^{2(\bullet+)}$ inclusion complex is supported by the relatively weak binding constant of between two $BIPY^{\bullet+}$ radical cations in the absence of the $CBPQT^{2(\bullet+)}$ ring to act as a "molecular flask". For detailed studies on the dimerization of $BIPY^{\bullet+}$ radical cation, see: Monk, P. M. S.; Hodgkinson, N. M.; Ramzan, S. A. *Dyes Pigm.* **1999**, *43*, 207.

(17) Li, H.; Fahrenbach, A. C.; Dey, S. K.; Basu, S.; Trabolsi, A.; Zhu, Z.; Botros, Y. Y.; Stoddart, J. F. *Angew. Chem., Int. Ed.* **2010**, *49*, 8260.

(18) Klajn, R.; Stoddart, J. F.; Grzybowski, B. A. *Chem. Soc. Rev.* **2010**, *39*, 2203.

(19) For examples of the use of organic radicals for the development of paramagnetic materials, see: Tretyakov, E.; Tolstikov, S.; Mareev, A.; Medvedeva, A.; Romanenko, G.; Stass, D.; Bogomyakov, A.; Ovcharenko, V. *Eur. J. Org. Chem.* **2009**, 2548.

(20) For examples of the use of organic radicals for the development of semiconductive matericals and device, see: (a) Usta, H.; Facchetti, A.; Marks, T. J. *Acc. Chem. Res.* **2011**, *44*, 501. (b) Nakahara, K.; Oyaizu, K.; Nishide, H. *Chem. Lett.* **2011**, *40*, 222. (c) Fahrenbach, A. C.; Sampath, S.; Late, D. J.; Barnes, J. C.; Kleinman, S. L.; Valley, N.; Hartlieb, K. J.; Liu, Z.; Dravid, V. P.; Schatz, G. C.; Van Duyne, R. P.; Stoddart, J. F. *ACS Nano* **2012**, *6*, 9964.

(21) All the [2]rotaxanes synthesized by radical templation, including **R′3**·$6PF_6$, **R′11**·$6PF_6$, and **R3**·$6PF_6$–**R11**·$6PF_6$, are thermodynamically unstable compounds, on account of the Coulombic repulsion between their mechanically interlocked components, affording these [2]rotaxanes higher ground-state co-conformational energies compared to their free dumbbell and ring components. In the cases of **R′11**·$6PF_6$ and **R3**·$6PF_6$–**R11**·$6PF_6$, their bulky stoppers result in sufficiently large steric barriers, preventing the deslippage of their ring components from their corresponding dumbbell component, on account of either the more remote distance between the charged components (in the case of **R′11**·$6PF_6$) or larger stoppers (in the case of **R3**·$6PF_6$–**R11**·$6PF_6$). In the case of **R′3**·$6PF_6$, its relatively small stoppers are unable to stop deslipping because of the enforced proximity between its $CBPQT^{4+}$ ring and the $BIPY^{2+}$ unit in the dumbbell component.

(22) We have demonstrated that the kinetic stability of a rotaxane-like entity is remarkably dependent on external conditions, such as the nature of solvent in which the compound is dissolved, implying that the cutoff between a pseudorotaxane and rotaxane is inherently imprecise and is best described using fuzzy sets. For details, see: Ashton, P. R.; Baxter, I.; Fyfe, M. C. T.; Raymo, F. M.; Spencer, N.; Stoddart, J. F.; White, A. J. P.; Williams, D. J. *J. Am. Chem. Soc.* **1998**, *120*, 2297.

(23) (a) Ashton, P. R.; Glink, P. T.; Stoddart, J. F.; Tasker, P. K.; White, A. J. P.; Williams, D. J. *Chem. Eur. J.* **1996**, *2*, 729. (b) Lutz, J.-F. *Angew. Chem., Int. Ed.* **2008**, *47*, 2182. (c) van Berkel, S. S.; Dirks, A. J.; Meeuwissen, S. A.; Pingen, D. L. L; Boerman, O. C.; Laverman, P.; van Delft, F. L.; Cornelissen, J. J. L. M.; Rutjes, F. P. J. T. *ChemBioChem* **2008**, *9*, 1805. (d) Becer, C. R.; Hoogenboom, R.; Schubert, U. S. *Angew. Chem., Int. Ed.* **2009**, *48*, 4900.

(24) (a) Hüisgen, R.; Szeimies, G.; Möbius, L. *Chem. Ber.* **1967**, *100*, 2494. (b) Kolb, H. C.; Finn, M. G.; Sharpless, K. B. *Angew. Chem., Int. Ed.* **2001**, *40*, 2004. (c) Tornoe, C. W.; Christensen, C.; Meldal, M. *J. Org. Chem.* **2002**, *67*, 3057. (d) Dichtel, W. R.; Miljanić, O. Š.; Spruell,

J. M.; Heath, J. R.; Stoddart, J. F. *J. Am. Chem. Soc.* **2006**, *128*, 10388. (e) Fahrenbach, A. C.; Stoddart, J. F. *Chem. Asian J.* **2011**, *6*, 2660.

(25) We have attempted to use a copper(I)-catalyzed azide−alkyne cycloaddition (CuAAC) to capture the mechanically interlocked structures of these [2]rotaxanes using radical templation. We have observed, however, that the Cu(I) catalyst oxidizes the $BIPY^{\bullet+}$ radical cation to the $BIPY^{2+}$ dication. This observation is supported by the fact that, upon addition of excess of the $Cu(MeCN)_4PF_6$ catalyst, the purple solution of $\mathbf{V3}^{\bullet+}\subset CBPQT^{2(\bullet+)}$ turns colorless.

(26) We have observed that the yields during the syntheses of the shorter [2]rotaxanes are relatively low in comparison with those for the longer ones, e.g., 5% for $\mathbf{R3}\cdot 6PF_6$ and 35% for of $\mathbf{R11}\cdot 6PF_6$. We hypothesize that the variation in yields results from intramolecular reductions of the terminal azide functions in the threads $\mathbf{V}(n+2)^{\bullet+}$ (n = 1−9) by their $BIPY^{\bullet+}$ radical cations, which act as competitive reactions to their 1,3-dipolar cycloadditions. We surmise that the rates of these azide reductions increase with the decrease in the distances between the $BIPY^{\bullet+}$ units and the terminal azide functions. This hypothesis is not unreasonable, considering our observation that a shorter counterpart of $\mathbf{R3}^{6+}$—bearing only two methylene units in each side of the dumbbell component—could not be prepared using a similar synthetic strategy.

(27) We observed that the monoradical state of [2]rotaxane $\mathbf{R3}^{6+}$, namely $\mathbf{R3}^{3(\bullet+)}$, is relatively stable under air for, i.e., atmospheric oxygen cannot oxidize $\mathbf{R3}^{(4+)(\bullet+)}$ to its fully oxidized state during a substantial amount of time (on the order of weeks). During the purification of the [2]rotaxane $\mathbf{R3}\cdot 6PF_6$, H_2O is employed in the final precipitation step. We reasonably assume that H_2O aides in the oxidation of the rotaxane to its fully oxidized form, namely $\mathbf{R3}^{6+}$. This assumption is supported by our observation that the purple solution of $\mathbf{R3}^{3(\bullet+)}$ turns colorless, upon addition of H_2O.

(28) Sutherland, I. O. *Annu. Rep. NMR Spectrosc.* **1971**, *4*, 71.

(29) The absolute values of ΔE obtained from DFT calculations are considerably higher than the $\Delta G^{\ddagger}_{c}$ values determined by ^1H NMR spectroscopy in solution. This observation results from the fact that the DFT calculations were performed, on the assumption that all the [2]rotaxanes are placed in a vacuum. In solution, the [2]rotaxane molecules are surrounded by polarizing solvent molecules—in particular, $(CD_3)_2CO$—which neutralize the positive charges on the [2]rotaxanes to some extent, thereby lowering the activation energy barriers to the shuttling of the $CBPQT^{4+}$ rings over the $BIPY^{2+}$ units in the corresponding dumbbells.

(30) We assume that the $BIPY^{2+}$ in the dumbbell component of the [2]rotaxane $\mathbf{R3}^{6+}$ has the highest tendency to be reduced, since this $BIPY^{2+}$ unit is encircled by a $CBPQT^{4+}$ ring and so experience Coulombic repulsion with both of the two $BIPY^{2+}$ units in the $CBPQT^{4+}$ ring. As a result, the first reduction peak observed at +0.10 V of the [2]rotaxane $\mathbf{R3}^{6+}$, can be assigned to the one-electron reduction of the $BIPY^{2+}$ unit in the dumbbell component ($BIPY^{2+}$/$BIPY^{\bullet+}$). This assumption is consistent with the DFT calculations based on the M06-2X/6-31G* level of theory.

(31) We have demonstrated recently (unpublished results) that a [2]catenane, comprised of two mechanically interlocked $CBPQT^{4+}$ rings, also undergoes stepwise two one-electron reductions, resulting in a monoradical state. This reaction results from the enforced close proximity of its four $BIPY^{2+}$ units on account of the mechanical bond, as in the case of $\mathbf{R3}^{6+}$.

(32) The mechanically interlocked nature of these [2]rotaxanes is responsible for the stabilization of their monoradical states in the gas phase, an assumption which is supported by a control experiment performed on $\mathbf{D3}\cdot 2PF_6$, where no molecular ion peak for $\mathbf{D3}^{\bullet+}$ was detected (see the SI) in the mass spectrum of $\mathbf{D3}\cdot 2PF_6$.

(33) The broad near-IR bands, centered on 1066 nm, are not observed in the UV/vis absorption spectra of the $(BIPY^{\bullet+})_2$ bisradical dicationic systems in which only two $BIPY^{\bullet+}$ radical cations are present in the radical-pairing interactions. For examples of these systems, see: (a) Geuder, W.; Hünig, S.; Suchy, A. *Tetrahedron* **1986**, *42*, 1665. (b) Jeon, W. S.; Kim, H.-J.; Lee, C.; Kim, K. *Chem. Commun.* **2002**, 1828.

(34) It has been reported that the $BIPY^{\bullet+}$ radical cationic monomer has a maximum absorption band centered on around 600 nm. For the UV/vis absorption spectra of $BIPY^{\bullet+}$ radical cation or $CBPQT^{2(\bullet+)}$ diradical dication, see ref 17.

(35) Shao, Y.; Molnar, L. F.; Jung, Y.; Kussmann, J.; Ochsenfeld, C.; Brown, S. T.; Gilbert, A. T. B.; Slipchenko, L. V.; Levchenko, S. V.; O'Neill, D. P.; DiStasio, R. A.; Lochan, R. C.; Wang, T.; Beran, G. J. O.; Besley, N. A.; Herbert, J. M.; Lin, C. Y.; Van Voorhis, T.; Chien, S. H.; Sodt, A.; Steele, R. P.; Rassolov, V. A.; Maslen, P. E.; Korambath, P. P.; Adamson, R. D.; Austin, B.; Baker, J.; Byrd, E. F. C.; Dachsel, H.; Doerksen, R. J.; Dreuw, A.; Dunietz, B. D.; Dutoi, A. D.; Furlani, T. R.; Gwaltney, S. R.; Heyden, A.; Hirata, S.; Hsu, C.-P.; Kedziora, G.; Khalliulin, R. Z.; Klunzinger, P.; Lee, A. M.; Lee, M. S.; Liang, W.; Lotan, I.; Nair, N.; Peters, B.; Proynov, E. I.; Pieniazek, P. A.; Rhee, Y. M.; Ritchie, J.; Rosta, E.; Sherrill, C. D.; Simmonett, A. C.; Subotnik, J. E.; Woodcock, H. L.; Zhang, W.; Bell, A. T.; Chakraborty, A. K.; Chipman, D. M.; Keil, F. J.; Warshel, A.; Hehre, W. J.; Schaefer, H. F.; Kong, J.; Krylov, A. I.; Gill, P. M. W.; Head-Gordon, M. *Phys. Chem. Chem. Phys.* **2006**, *8*, 3172.